



Nonlinear three-mode interactions in a developing mixing layer

D. E. Nikitopoulos and J. T. C. Liu

Citation: [Physics of Fluids](#) **13**, 966 (2001); doi: 10.1063/1.1351857

View online: <http://dx.doi.org/10.1063/1.1351857>

View Table of Contents: <http://scitation.aip.org/content/aip/journal/pof2/13/4?ver=pdfcov>

Published by the [AIP Publishing](#)

Articles you may be interested in

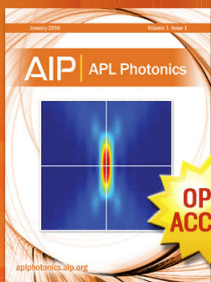
[Novel features of a fully developed mixing-layer between co-flowing laminar and turbulent Couette flows](#)
Phys. Fluids **26**, 031703 (2014); 10.1063/1.4868645

[Global and Koopman modes analysis of sound generation in mixing layers](#)
Phys. Fluids **25**, 124101 (2013); 10.1063/1.4834438

[Linear and nonlinear instability waves in spatially developing two-phase mixing layers](#)
Phys. Fluids **22**, 052103 (2010); 10.1063/1.3425788

[The dynamics of nonlinear instability waves in laminar heated and unheated compressible mixing layers](#)
Phys. Fluids **21**, 094103 (2009); 10.1063/1.3232329

[Passive scalar mixing in a planar shear layer with laminar and turbulent inlet conditions](#)
Phys. Fluids **14**, 985 (2002); 10.1063/1.1445421



Launching in 2016!

The future of applied photonics research is here

OPEN
ACCESS

AIP | APL
Photonics

Nonlinear three-mode interactions in a developing mixing layer

D. E. Nikitopoulos^{a)}

Mechanical Engineering Department, Louisiana State University, Baton Rouge, Louisiana 70803

J. T. C. Liu^{b)}

Institut für Aero- und Gasdynamik, Universität Stuttgart, Pfaffenwaldring 21, 70550 Stuttgart, Germany

(Received 25 June 1999; accepted 9 January 2001)

A formulation based on the integral energy method is presented for the nonlinear interaction problem between three large-scale coherent modes in a developing, laminar, free shear layer. Both binary and three-mode nonlinear, modal energy and phase interactions are included. The modal evolution and the development of the mean flow are very sensitive to the initial energy contents and phases of the participating modes. A strong nonlinear coupling of the modal phase variations with the variations of the modal energies is shown to exist and is responsible for the rapid reversal of the intermodal energy interactions in favor of the occasionally declining mode. This nonlinear mechanism preserves the higher frequency modes far downstream and is shown to contribute to the appearance of mean flow contraction observed in experiments through local collective return of energy to the mean by all modes. Depending on initial conditions, our results support the arguments of R. A. Petersen and R. C. Clough [“The influence of higher harmonics on vortex pairing in an axisymmetric mixing layer,” *J. Fluid Mech.* **239**, 81 (1992)] and M. R. Hajj, R. W. Miksad, and E. J. Powers [“Subharmonic growth by parametric resonance,” *ibid.* **236**, 35 (1992)] according to which three-mode resonances are more efficient than the binary ones. Two cases relevant to situations where the first and second subharmonics of the most amplified mode are forced involving the 3/2 harmonic and 2/3 subharmonic, respectively, are examined. Comparisons of the calculations with experimental results indicate good qualitative agreement. © 2001 American Institute of Physics. [DOI: 10.1063/1.1351857]

I. INTRODUCTION

Following the experiments of Refs. 1 and 2 large-scale coherent structures have been widely accepted as intrinsic features of transitional free shear flows. One of the prevailing trends of thought is to interpret them as wave-like structures, products of hydrodynamic instability in an inflectional mean flow, superimposed upon fine-grained turbulence.^{3,4} According to nonlinear hydrodynamic instability ideas,⁵ coherent structures have been associated with waves modulated by amplitudes whose variation is much slower than the wave oscillation. Experiments such as those of Ref. 6 have shown that the local characteristics of these waves are well represented by local linear stability theory. The evolution of the flow is governed by mutual nonlinear interactions between the mean flow, the wave-like large-scale structures and the fine-grain turbulence.⁷ Experimental evidence suggests that the frequency associated with the wave-like, large-scale structure most often observed in “natural” shear layers (subject only to naturally-occurring, low-level, broad-band noise) is in good agreement with the most amplified frequency as predicted by linear stability analysis.^{8,9} Periodic excitation of the large-scale structure has often been used as a tool to

explore the physics of the flow and as a means to achieve some level of flow-control for practical purposes. By using artificial excitation, experiments such as those of Refs. 10 and 11 have examined the role of subharmonics of the most amplified (fundamental) frequency and their relationship to the observed vortex-pairing and shredding phenomena. Experimental evidence^{12–16} also supports theoretical predictions^{16–20} indicating that the downstream development of the large-scale structures, and the flow in general, strongly depends on initial conditions. This has been particularly evident when subharmonic forcing has been used, and a number of results from experiments^{12,21} numerical simulations^{22,23} and theoretical studies^{17,18,24,25} have shown that the relative phase of the fundamental and subharmonic is a determining factor of the intramodal energy transfer. The nonlinear interaction mechanism that exchanges energy between the fundamental and subharmonic modes is not the predominant one in the development of the subharmonic far downstream when compared to the interaction with the mean flow.¹⁷ Nevertheless, the contribution of the additional indirect effects of this binary modal interaction on the energy exchange with the mean flow, make the former mechanism one of considerable importance. However, the fundamental and subharmonic modes are not the only ones of significant magnitude in the flow. This is particularly true when forcing has been used. There is ample experimental evidence attesting to this in the work of Ref. 10; in both cases of their modes I and II a frequency at 3/2 of the most amplified one was strong

^{a)}Author to whom correspondence should be addressed. Telephone: 225-578-5903; Fax: 225-578-5924; electronic mail: meniki@me.lsu.edu

^{b)}On sabbatical leave during 2000/01. Permanent address: Division of Engineering and the Center for Fluid Mechanics, Brown University, Providence, Rhode Island 02912.

enough to be reported and an inspection of their measured spectra also shows the presence of higher harmonics. The work of Ref. 15 has also shown a strong presence of harmonics in excited shear layers and have related to their existence the observed local contraction of the shear layer. It has also been argued by Weisbrot and Wagnanski that a Kelly²⁴ type resonance may occur between the fundamental and first harmonic. Experimental evidence from shear layers in backward facing steps²⁶ have also shown a strong presence of harmonics far downstream. Petersen and Clough²⁷ pointed out that the leading resonant interaction in their experiments conducted on a forced axisymmetric shear layer, is one involving the $3/2$ harmonic, the fundamental and the subharmonic, rather than the last two alone. In their study, higher harmonics were also found to influence the growth of the fundamental and subharmonic modes. The presence of harmonics of the fundamental mode in the flow is not surprising given that the first harmonic can be produced from the fundamental by self-interaction, a $3/2$ harmonic can be produced from the binary interaction between the subharmonic and the fundamental and a broad family of frequencies higher than the fundamental can be subsequently produced from the mutual interactions between these modes. From the linear stability point of view, of all the harmonics of the most amplified mode, the $3/2$ one is the most likely to persist, since it is the only one capable of drawing energy from the mean flow while the fundamental is still amplified. The first harmonic is in the neighborhood of neutral stability when the fundamental experiences maximum amplification, while higher harmonics are being dampened by losing energy to the mean flow. This is true for all velocity ratios of the shear layer as evidenced from the stability curves of Ref. 9. In view of the experimental observations showing that harmonics persist far downstream after the fundamental and the subharmonic have peaked, it is reasonable to assume that their longevity can be attributed, at least partially, to energy channeled to them from the fundamental and the subharmonic modes through nonlinear interactions. On the basis of energy equations for odd and even modes, as formulated by Refs. 28 and 17, the fundamental can interact with its first subharmonic and its first harmonic directly through a two-wave interaction, while the $3/2$ harmonic can only interact with the fundamental and/or the subharmonic through a three-wave interaction mechanism. Any interaction involving two modes, one having twice the frequency of the other, falls in the class discussed by Refs. 24, 25, and 17. Such is the case of the interaction between the fundamental and its first harmonic as pointed out by Ref. 15. Unlike three-mode interactions, these binary interactions have attracted a good deal of attention thus far, since they were the first ones identified as relevant to subharmonic development and the associated vortex merging and shredding phenomena. In order to investigate the role of harmonics, particularly the $3/2$ one, and their interactions with the fundamental and subharmonic modes, and in view of the observations of Ref. 27, it is necessary to take three-mode interactions into consideration. Furthermore, three-mode interactions are also relevant to cases where higher order subharmonics of the most amplified frequency are forced, whereby intermediate frequencies as well as har-

monics are likely to be important. An example of such a case is that of mode III in the experiments of Ref. 10, where the second subharmonic of the most amplified fundamental mode was forced and an intermediate frequency at $2/3$ that of the fundamental appeared in considerable strength. These three frequencies can be coupled via binary and three-mode interactions, the latter being the only means of energy communication between the second subharmonic and the fundamental. In establishing this communication, the brokerage of the intermediate $2/3$ mode is essential.

The present study is concerned with the evolution of three interacting wave modes in a laminar shear-layer, taking into account both binary and three-wave interactions. The two cases that will be considered here are most likely to arise when low amplitude forcing of the first subharmonic, and the second subharmonic of the most amplified frequency is individually applied to the shear layer. The role of the $3/2$ harmonic on the evolution of the subharmonic and fundamental through three-mode interactions is examined in the first case, while the role of the intermediate $2/3$ mode is considered in the second case. The effect of initial conditions and the relative importance of three-wave and binary interactions and the related resonances is discussed for these two representative cases. A modified integral energy method originating from Ref. 29 is used in this analysis. This method has been used with success in the past to study the nonlinear development of laminar wakes,³⁰ free shear layers,^{17,18} and round jets.^{19,20,31} By virtue of the energy method the original set of partial differential equations governing the evolution of the mean flow and the large-scale modes is reduced to a set of ordinary nonlinear differential equations for the mean flow thickness, the modal energies, and the modal phases.

Prior to proceeding with the integral energy formulation used for the purposes of this study, it is in order to discuss another powerful nonlinear perturbation approach that has also been used successfully to further the understanding of the nonlinear dynamics of shear flows. In a series of two papers, Goldstein and co-workers studied the externally excited mixing layer from a local nonlinear, nonequilibrium critical layer point of view for which the flow within the cat's eyes need not be uniform. In their study³² an inviscid analysis is performed and the case is considered where the deviation of the Strouhal frequency (normalized by the local shear layer thickness) from its neutral value for the fundamental component is large compared to the wave amplitude, measured by $\sqrt{\epsilon}$ and ϵ , respectively. The resulting lowest order vorticity equation for the critical layer has both effects of nonlinearity and inertia thus rendering its solution to be matchable to the upstream linear instability wave solution. They used a composite expansion procedure to obtain a single relation that accounts for effects of shear layer growth and nonlinearity in the critical layer. Though a rational approach, the expansion procedure is dependent upon a "small" amplitude assumption. The fundamental component was the primary disturbance. The first harmonic component, with amplitude necessarily smaller than the fundamental because of the assumptions leading to the expansion procedure, appears to be the strongest among the harmonic components, while subharmonics were not considered. In the inviscid

analysis, Ref. 32 did not make an explicit graphical comparison between their Reynolds-stress induced additional shear layer growth with that of the shear layer growth of Ref. 10. Because their analysis was inviscid, they used a “normalized” shear layer thickness value in terms of a percentage deviation from the local undisturbed viscous growth and showed that its value was consistent with experiments¹⁰ in the region where the fundamental component is near its local neutral. In the subsequent viscous critical layer analysis,³³ no further comments were made on the shear layer growth. In Goldstein and Leib’s³² explicit plot, their shear-layer momentum thickness increased to a maximum and then decayed. The typical “plateau” regions reached in Ho and Huang’s experiments were not recovered. This could be, in view of the present paper, because subharmonics were not present in their analysis. It subsequently³⁴ generalized the previous analyses from a hyperbolic tangent profile to an arbitrary mean velocity profile (to partially account for the possible wake effect behind the trailing edge of the exit flow). He analyzed the next stage of the influence on the instability wave development by both the shear layer growth and nonlinear critical layer effects. He also generalized the inviscid streamwise composite solution of Ref. 32 to include viscosity effects. Hultgren³⁴ compared the results of the analysis with three sets of experiments:³⁵ in the initial region of a plane jet,³⁶ in the initial region of a round jet, and Ho and Zohar whose results eventually appeared in Ref. 37. The comparisons, in terms of a shear layer thickness and fluctuation amplitude, are limited to two regions for which the theory is valid, namely, (1) in the linear fluctuation region, in which the shear growth due primarily to viscous effects where the Reynolds stresses of the fluctuations are too small to influence the shear layer and (2) in the downstream region where the fundamental component (and its “weak” nonlinear harmonics) dominated. Region (1) showed that the weakly nonparallel theory compared well. The comparisons in the initial nonlinear region showed reasonable agreement with experiments prior to the dominance of subharmonics not present in the analyses.³⁴

The present triple mode interaction problem essentially derives its basic formulation from the single mode formulation of Ref. 30, in that the shape assumption ideas of Ref. 29 were extended to developing shear flows using the integrated form of kinetic energy and momentum equations for the mean motion and kinetic energy equations for the fluctuating components. The relative amplitudes of the fluctuations need not necessarily be small; each fluctuation component has its own inertia and is coupled to other fluctuating components and the mean motion through nonlinear effects of energy exchange. This is in contrast to the rational but necessarily “weak” nonlinear analyses^{38,32–34} in which the fluctuations are expanded in ascending powers of the (fundamental) amplitude. It should be noted that Goldstein’s approach does not rely on a local linear assumption and that the mode shapes resulting from his analysis bear explicit nonlinear effects. However, although the cross-stream shapes of the modes considered by the present formulation are products of local linear analysis, the cross-stream shapes of the composite perturbation (including all modes considered) bears im-

plicit nonlinear effects through the weight of the nonlinearly determined modal amplitude and phases. Finally, the present approach enables investigation of subharmonic dynamics, which are not included in the analyses of Goldstein and co-workers.

II. FORMULATION

The problem under consideration is a spatial one involving the simultaneous determination of the streamwise development of the mean flow and the large-scale structure. All variables are made dimensionless using the average velocity of the two free streams, U , as the velocity scale, and one half the vorticity (or maximum slope) thickness, δ , as the length scale. Every flow quantity is decomposed into a mean motion component, q^0 , and a wave, associated with the large-scale structure as in Refs. 17 and 18. The large-scale structure is assumed to evolve in the streamwise direction and to be periodic in time. It is further decomposed into discrete modes,

$$\tilde{q}(\mathbf{x}, t) = \sum_k [q^n(\mathbf{x}; n\beta) e^{-in\beta t} + q^{-n}(\mathbf{x}; n\beta) e^{in\beta t}], \quad (1)$$

where q^{-n} is the complex conjugate of q^n , $\beta = 2\pi f\delta(x)/U$ is the local dimensionless frequency (Strouhal number), f is the physical frequency, and k is the number of modes that are, either naturally or by means of forcing, present in the flow. The local Strouhal number is implicitly a function of the streamwise coordinate through its dependence on the local maximum slope thickness. In this study we will consider three modes of frequencies, $\beta_1 = \beta$, $\beta_2 = 2\beta$, and $\beta_3 = 3\beta$. We shall seek to investigate the effects of interactions between these three modes on the development of an otherwise laminar, viscous shear flow. Our analysis focuses into the initial region of development of a shear layer whose initial small-scale turbulence level is low. Therefore, interactions with the fine-grain turbulence, previously studied by Refs. 39 and 40 have not been included.

Equations of motion for each flow component, including the three discrete wave-modes, are derived from the Navier–Stokes and continuity equations for incompressible flow by straight forward manipulations and use of time-averaging. Kinetic energy equations, for the mean flow, and each mode individually, are then derived from these as in Ref. 17. The mean-flow kinetic energy equation is

$$\begin{aligned} \frac{\bar{D}}{Dt} \left(\frac{(u_i^0)^2}{2} \right) &= \frac{\partial u_i^0}{\partial x_j} \sum_1^3 \Re(u_i^k u_j^{-k}) \\ &+ \frac{1}{\text{Re}} \left[\frac{\partial^2}{\partial x_j \partial x_j} \left(\frac{(u_i^0)^2}{2} \right) - \frac{\partial u_i^0}{\partial x_j} \frac{\partial u_j^0}{\partial x_i} \right] + \dots \end{aligned} \quad (2)$$

The first term on the right-hand side represents the energy exchange mechanism between the mean flow and the three modes collectively. Depending on its sign, energy can flow to or from the mean flow at the expense or gain of the wave component. The same interpretation holds for the individual modes. The energy equations for the three modes, put in a single equation, are

$$\begin{aligned}
u_j^o \frac{\partial}{\partial x_j} \left(\frac{|u_i^n|^2}{2} \right) = & - \frac{\partial u_j^o}{\partial x_j} \Re(u_i^n u_j^{-n}) + \frac{1}{\text{Re}} \left(\frac{\partial^2}{\partial x_j \partial x_j} \left(\frac{|u_i^n|^2}{2} \right) - \left| \frac{\partial u_i^n}{\partial x_j} \right|^2 \right) + \delta_{3n} \Re \left(u_i^2 u_j^1 \frac{\partial u_i^{-3}}{\partial x_j} + u_i^1 u_j^2 \frac{\partial u_i^{-3}}{\partial x_j} \right) \\
& + \delta_{2n} \Re \left(u_i^{-1} u_j^3 \frac{\partial u_i^{-2}}{\partial x_j} - u_i^2 u_j^1 \frac{\partial u_i^{-3}}{\partial x_j} + u_i^1 u_j^1 \frac{\partial u_i^{-2}}{\partial x_j} \right) \\
& + \delta_{1n} \Re \left(-u_i^1 u_j^2 \frac{\partial u_i^{-3}}{\partial x_j} - u_i^{-1} u_j^3 \frac{\partial u_i^{-2}}{\partial x_j} - u_i^1 u_j^1 \frac{\partial u_i^{-2}}{\partial x_j} \right) + \dots, \quad \forall n \in [1, 3],
\end{aligned} \quad (3)$$

where \Re is the real part function, $\|$ denotes magnitude, and δ_{kn} is the Kronecker delta. In both Eqs. (2) and (3) “redistribution” terms have been omitted for the sake of brevity. The first term on the right-hand side is the energy exchange of mode n with the mean flow. The last three groups of terms provide the intermode coupling. Each member of every group represents work done by wave-induced stresses against modal rates of strain. The direction of the energy transfer depends on the sign of these terms, controlled by the relative modal phases. Modes β and 2β can exchange energy directly through a binary interaction and can be independent of mode 3β . Two-mode interaction problems in free shear flows have been studied by Refs. 17 and 19, among others, assuming that the phase of each mode varies according to linear theory. Subsequent experimental evidence of Ref. 41 has indicated that the variation of the phases is highly nonlinear, and several studies have been conducted since, taking into account such nonlinear variation of the phases.^{18,31,42} Thus, in order to properly address the problem, governing equations for the modal phases are also derived from the equations of motion. Details of the derivation method can be found in any of the three studies mentioned previously. Put in single equation form, the equations for the phase of mode n are given by

$$\begin{aligned}
\frac{1}{2} u_j^o \frac{\partial}{\partial x_j} \ln \left(\frac{u_i^n}{u_j^{-n}} \right) = & - n \beta |u_i^n|^2 - \frac{\partial u_j^o}{\partial x_j} \Im(u_i^n u_j^{-n}) + \frac{1}{\text{Re}} \Im \left(\frac{\partial}{\partial x_j} \left(u_i^{-n} \frac{\partial u_j^n}{\partial x_j} \right) \right) + \delta_{3n} \Im \left(u_i^2 u_j^1 \frac{\partial u_i^{-3}}{\partial x_j} + u_i^1 u_j^2 \frac{\partial u_i^{-3}}{\partial x_j} \right) \\
& + \delta_{2n} \Im \left(u_i^{-1} u_j^3 \frac{\partial u_i^{-2}}{\partial x_j} + u_i^2 u_j^1 \frac{\partial u_i^{-3}}{\partial x_j} + u_i^1 u_j^1 \frac{\partial u_i^{-2}}{\partial x_j} \right) \\
& + \delta_{1n} \Im \left(u_i^1 u_j^2 \frac{\partial u_i^{-3}}{\partial x_j} - u_i^{-1} u_j^3 \frac{\partial u_i^{-2}}{\partial x_j} + u_i^1 u_j^1 \frac{\partial u_i^{-2}}{\partial x_j} \right) + \dots, \quad \forall n \in [1, 3],
\end{aligned} \quad (4)$$

\Im denoting the imaginary part. The evolution of the phases is affected by the mean flow (second term on the right-hand side) as well as the intramode coupling (last three groups of terms). The first and third terms on the right-hand side are the temporal and viscous contributions, respectively.

A. Shape assumptions

We are presently considering the problem posed by the existence of two-dimensional wave-modes in a two-dimensional, yet self-similar, mean flow. The mean flow profile is assumed to be adequately represented by a traditional hyperbolic tangent profile,

$$u^o(\eta) = 1 - R \tanh(\eta), \quad (5)$$

characterized by a velocity ratio $R = (U_{-\infty} - U_{+\infty}) / (U_{-\infty} + U_{+\infty})$, where $U_{-\infty}$ and $U_{+\infty}$ are the fast and slow stream velocities, respectively, and $\eta = y / \delta(x)$ is the dimensionless cross-stream coordinate scaled with the local maximum-slope thickness. This profile has been experimentally verified in the developed region by numerous experiments^{10,43} and used in several previous studies.^{17,18,39,40} The choice of this profile is made assuming that distortion of the mean flow due to the large-scale structure presence is negligible. For the purposes of the present study a profile with $R = 0.31$ has been used, in accordance to the experiments of Ref. 10.

According to previous work by Refs. 16–18,29,30 the two components of the large-scale modal Fourier amplitudes, u^n , v^n , of the velocity in Eqs. (2), (3), and (4) are assumed to be separable into an unknown finite complex amplitude and corresponding vertical shape functions,

$$\begin{bmatrix} u^n(\mathbf{x}, t) \\ v^n(\mathbf{x}, t) \end{bmatrix} = |A_n(x)| e^{i\psi_n(x)} \begin{bmatrix} \phi_n'(\eta) \\ -i\alpha_n \phi_n(\eta) \end{bmatrix}. \quad (6)$$

The amplitude magnitude, $|A_n(x)|$, and phase angle, $\psi_n(x)$, are to be determined jointly with the maximum slope thickness, $\delta(x)$, from the mean energy Eq. (2), wave mode energy Eqs. (3), and phase angle Eqs. (4). Previous investigations employing nonlinear or weakly nonlinear analyses have used factors, involving the streamwise complex wave number α_n , equal to $\exp(i\alpha_n x)$ or $\exp(i\int_0^x \alpha_n d\xi)$ (e.g., Ref. 44) in definitions similar to that of (6). This has been done to take into account the variation of the amplitude as accepted in linear stability analysis, which is valid while its magnitude is still very small and nonlinear effects are not important. We have not introduced such factors here since we have developed explicit nonlinear, governing equations for both the magnitude and phase of the complex amplitude. The shape function, $\phi_n(\eta)$, in (6) is evaluated together with the complex wave number, α , by solving the local linear, inviscid, eigenvalue problem for a single mode governed by the Rayleigh equation. Solutions of the linear problem are obtained

well into the dampened region ($\beta > 1$) by using a complex contour integration scheme previously used by Ref. 17 to take care of the singularity of the equation. The inviscid problem is adequate for our purposes since the mean velocity profile is inflectional and therefore dynamically unstable. The eigenfunctions are normalized so that (a) their phases are zero at the point of maximum slope, and (b) $|A_n(x)|^2$ is related to the corresponding modal energy density by

$$E_n(x) = \frac{1}{2} \int_{-\infty}^{+\infty} ((u^n)^2 + (v^n)^2) dy = |A_n(x)|^2 \delta(x). \quad (7)$$

B. Integral equations

Equations (2)–(4) are integrated across the shear layer. After introducing the shape assumptions, and with the aid of boundary-layer-type approximations we then obtain the following set of nonlinear, differential equations for the modal energy densities, E_n , modal phases, ψ_n , and the mean flow thickness,

$$\begin{aligned} \delta \frac{I_n}{E_n} \frac{dE_n}{dx} = & I_{Mn} - \frac{I_{Dn}}{\text{Re}_0 \delta} + E_1 \sqrt{\frac{E_2}{\delta}} \left(\frac{\delta_{1n}}{E_1} - \frac{\delta_{2n}}{E_2} \right) I_{12}^1 \\ & + \sqrt{\frac{E_1 E_2 E_3}{\delta}} \left[\left(\frac{\delta_{1n}}{E_1} - \frac{\delta_{2n}}{E_2} \right) I_{12}^3 \right. \\ & \left. + \left(\frac{\delta_{1n}}{E_1} - \frac{\delta_{3n}}{E_3} \right) I_{13}^2 + \left(\frac{\delta_{2n}}{E_2} - \frac{\delta_{3n}}{E_3} \right) I_{23}^1 \right], \quad (8) \end{aligned}$$

$$\begin{aligned} 2\delta I_n \frac{d\psi_n}{dx} = & 2n\beta\delta + P_{Mn} - \frac{P_{Dn}}{\text{Re}_0 \delta} + E_1 \sqrt{\frac{E_2}{\delta}} \left(\frac{\delta_{1n}}{E_1} \right. \\ & \left. + \frac{\delta_{2n}}{E_2} \right) P_{12}^1 + \sqrt{\frac{E_1 E_2 E_3}{\delta}} \left[\left(\frac{\delta_{2n}}{E_2} - \frac{\delta_{1n}}{E_1} \right) P_{12}^3 \right. \\ & \left. + \left(\frac{\delta_{3n}}{E_3} + \frac{\delta_{1n}}{E_1} \right) P_{13}^2 + \left(\frac{\delta_{3n}}{E_3} + \frac{\delta_{2n}}{E_2} \right) P_{23}^1 \right], \quad (9) \end{aligned}$$

$$\delta I_M \frac{d\delta}{dx} = \sum_1^3 (E_k I_{Mk}) + \frac{I_D}{\text{Re}_0}, \quad \forall n \in [1, 3]. \quad (10)$$

The energy equation is written in amplification-rate form. Note that the modal equations are in a form identical to those developed by Ref. 45 and used by Ref. 21 as the basis for their transfer function equation. The lengths in the above equations have been rescaled by the initial thickness, δ_0 , of the shear layer at the onset of the self-similar region; thus the initial Reynolds number is defined as $\text{Re}_0 = \delta_0 U/v$. The mean-flow integral coefficients I_M (mean advection) and I_D (mean dissipation) are constant and positive, while those involving a single wave mode I_n (modal advection), I_{Mn} , P_{Mn} (interaction with the mean flow), and I_{Dn} (modal dissipation) depend on $\delta(x)$ through the dependence of the local shape functions of the modes on the local frequency $\beta(x)$. The definitions of these integral coefficients can be found in the Appendix. The mean advection integral is a very weak function of β and has been fixed at a constant value approximately equal to unity. The integral representing the interaction between the mean flow and each of the wave-modes (I_{Mn}) is positive for frequencies lower than the neutral one

and energy is transferred from the mean flow to the corresponding wave-mode. As a result of this interaction, the mean flow grows fast while the wave-mode is amplified. The magnitude of I_{Mn} typically increases with increasing frequency in the amplified region, reaches a maximum at the most amplified frequency, and then declines towards zero near the neutral frequency.¹⁷ Beyond the neutral point the sign of this integral and the direction of the energy flow is reversed and the wave-mode is dampened by returning energy to the mean flow. When only one wave-mode is present in the dampened region, according to Eq. (10), the laminar shear layer will continue growing slowly at a much reduced rate maintained by viscosity, even as the wave-mode is returning energy to the mean flow, provided that the energy density, E_n , of the single mode satisfies the condition $E_n < (4R^2)/(3\text{Re}_0|I_{Mn}|)$. This condition is usually satisfied given that (a) the right-hand side of the inequality is very large near the neutral point, (b) the modal energy is much less than unity, and (c) both sides diminish further into the dampened region. Furthermore, in the case of a turbulent shear layer, the action of small-scale turbulence further promotes the mean flow growth and thus it is very unlikely that the return of energy to the mean flow by a single prominent large-scale mode may cause mean growth reversal. In the presence of a fundamental and subharmonic mode, as in the case examined by Ref. 17, the fast growth of the mean flow is resumed after the fundamental saturates because of the peak energy drain from the mean flow caused by the amplified subharmonic. Far downstream, when both modes are returning energy to the mean, the appearance of mean flow contraction is likely, provided that the fundamental mode has sustained some of its strength. As shown in Ref. 17, the fundamental can preserve its strength in the dampened region through a favorable nonlinear interaction with the subharmonic. However, mean flow contraction was not observed in any of the binary interaction cases examined in their study. Contraction of the mean flow becomes more likely in the presence of multiple modes that are being dampened by collectively returning energy to the mean flow and overpowering the growth driven by viscosity and small-scale turbulence, particularly when the latter is weak. Such appears to be the case in the experiments of Ref. 15, where the fundamental and harmonics maintain their strength in the region (region II in their paper) where the mean flow contraction is observed. Modes that are being dampened by losing energy to the mean flow can only be sustained by nonlinear interactions with other modes while the latter are being amplified. Therefore it is expected that the existence of such interactions is intimately related to the observed mean flow contraction.

In the present case of study, the nonlinear energy interactions between the three modes considered are represented by the last two terms of Eq. (8) while the nonlinear interactions affecting the phases are represented by the last two terms of Eq. (9). The interaction coefficients I_{jk}^n , and P_{jk}^n are defined as the real and imaginary part, respectively, of complex interaction coefficients expressed as

$$S_{nj}D_k = |S_{nj}D_k| \exp(i\Psi_{jk}^n), \quad (11)$$

and given explicitly in the Appendix. Since the nonlinear interaction terms result from products of wave-stresses and wave-strain-rates, the total phase angle, Ψ_{jk}^n , of the interaction integrals is a measure of the degree of alignment of the local wave-stress involving modes n and j and the wave-strain-rate of mode k . This is so in an “integral sense” because of the averaging process that has been applied. The magnitude and phase of each of these complex interaction coefficients are implicitly functions of the streamwise coordinate through their explicit dependence on the local dimensionless frequencies β_n . The total phase angles also depend explicitly on the local phases, ψ_n , which vary nonlinearly with the streamwise coordinate. Thus, the total phase angle of the binary interaction coefficient depends on $\theta = (\psi_2 - 2\psi_1)$ and can be written as $\Psi_{12}^1 = \theta + \xi_{12}^1$ while the total phase angle of the three-mode interaction coefficients depends on $\varphi = (\psi_3 - \psi_2 - \psi_1)$ and can be written as $\Psi_{jk}^n = \varphi + \xi_{jk}^n$ (for $n \neq j \neq k$). The quantities ξ_{jk}^n are the contributions to the total phase angle coming from the integrals contained in the complex interaction coefficients, that are calculated using the local linear stability eigenfunctions and therefore depend implicitly on the local Strouhal numbers of the modes. The magnitudes, $|S_{nj}D_k|$, of the interaction coefficients depend only on the local Strouhal numbers and are thus implicit functions of the streamwise coordinate. According to the calculations based on the mean velocity profile with $R=0.31$, these magnitudes are approximately of the same order (10^{-1}) for all four modal interactions over a wide range of the frequency ($\beta \leq 1.5$). The weakest one is $|S_{31}D_2|$, which affects the interaction between modes 1 and 2, while $|S_{21}D_3|$ affecting the interaction between modes 1 and 3 is the strongest. It is worth mentioning that the binary interaction coefficient is not the strongest one in the group. The magnitude of the interaction terms themselves is primarily controlled by the corresponding amplitudes and total phase angles of the modes involved. The latter also control the direction of the energy transfer. For given modal amplitudes maximum energy interaction between modes j and k occurs when the magnitude of the interaction coefficient I_{jk}^n is maximized. This happens when the corresponding total interaction phase angle, Ψ_{jk}^n , is an integer multiple of π , and the relevant wave stress is aligned with the corresponding strain-rate on an average basis. Under this condition, the nonlinear interaction affecting the phases of modes j and k is nullified. The phase interaction is maximized when Ψ_{jk}^n is an odd multiple of $\pi/2$, in which case, the energy interaction is nullified and the relevant wave stress and strain-rate are orthogonal. The intra-modal energy interactions and phase interactions are reversed when the corresponding total interaction phase angles cross an odd multiple of $\pi/2$ and an integer multiple of π , respectively. Thus, when Ψ_{jk}^n is in the fourth and first quadrants the interaction coefficient I_{jk}^n is positive and energy flows from mode k to mode j according to Eq. (8), while the opposite is true when the total interaction phase angle is in the second and third quadrants. For example, in the case of the binary interaction which is influenced by I_{12}^1 , the energy flow from mode 2 to mode 1 is maximized when $\Psi_{12}^1 = 0$.

It is seen from Eqs. (8) and (9) that in addition to the direct, binary interaction between modes 1 and 2, three indirect, three-mode interactions establish communication between the three modes considered here. Through such indirect interactions, mode 3 is coupled with modes 1 and 2, and also contributes to a second channel of communication between the latter two.

The interaction term with the mean flow is the leading term in Eq. (8) for the modal energy amplification rate. Its sign and magnitude dictates the growth rate of the energy of each mode provided that it dominates the cumulative contribution of the interactions with other modes. If not, it is possible that a given mode is dampened because of its interactions with other modes, while it is still extracting energy from the mean flow. The opposite is also possible. The term representing the interaction between modes j and k with the participation of mode n is proportional to a factor $\sqrt{E_n E_k / E_j}$ in the j -energy equation and $\sqrt{E_n E_j / E_k}$ in the k -energy equation. Thus, a key feature of the mode interactions is that a “weaker” mode can experience a considerable boost in the rate of amplification or dampening by interacting with a “stronger” one, at little expense or gain of the amplification rate of the latter.

In the modal phase Eq. (9) the most significant term is the first one on the right-hand side, which together with the mean interaction (second term) reflects the local, linear, inviscid contribution to the modal phase gradient. In the absence of intramodal, nonlinear interactions, $d\psi_n/dx$ is by definition equal to the real part of the eigenvalue α_n . The phase interaction terms, although weaker in general, can be very important. It is observed in Eq. (9) that most of the phase interactions tend to shift the phases of the interacting modes in the same direction, with the exception of the indirect interaction between modes 1 and 2. As in Eq. (8) the phase interaction terms in the phase equation of mode j are proportional to the same factor $\sqrt{E_n E_k / E_j}$. Consequently, the phase interaction terms can become quite significant when the energy of the mode whose phase is affected becomes very small compared to the energies of the other participating modes. Thus a nonlinear mechanism exists that can introduce violent modal phase shifts. Such phase shifts can have a profound effect on the total interaction phase angles and thus affect both the magnitude and direction of the energy interactions as well as those of the phases. This mechanism can also lead to rapid tuning or detuning of modal interactions.

Equations (8)–(10) are subject to a multitude of “initial” conditions at the onset of the shear layer. With three modes present, these include three initial modal energy densities (E_{n0}) and phases (ψ_{n0}), and the frequency parameter $\beta_0(\delta_0)$. The development of the wave-modes and the mean flow will depend on these initial conditions. The modal interaction terms in particular are affected by the initial values of the phase angle differences θ_0 and φ_0 which depend on the initial modal phases ψ_{n0} . Therefore the initial values of the former rather than the latter are going to be used to characterize each case examined in the sections that follow.

III. DISCUSSION AND RESULTS

A. Interactions involving mode $3\beta/2$

We will examine in this section the mutual interactions of three wave modes with initial frequencies $\beta_0/2$, β_0 , and $3\beta_0/2$, where the initial frequency of the fundamental β_0 is approximately equal to β_m the most amplified frequency for the given mean-flow profile with a velocity ratio of 0.31 according to linear stability analysis. This situation arises when subharmonic forcing of the shear layer is used (e.g., Refs. 10, 11, 21, 27) and the $3\beta_0/2$ harmonic can be generated from the interaction of the subharmonic with the fundamental. Of course higher harmonics (2β , 3β , etc.) can be produced, as indicated by the experimental studies listed above and the theoretical study of Ref. 18. The latter showed that the first and second harmonics of the fundamental are produced and sustained downstream through nonlinear interaction with the fundamental. The study of Ref. 21, in particular, has confirmed this indicating that the second harmonic is produced downstream via self-interaction of the fundamental. However, from the point of view of the present study which focuses on the subharmonic, such modes, as well as the intermediate $5\beta/2$, will be of lesser importance than the presently considered $3\beta/2$. The significance of this mode is that it can produce the subharmonic with the aid of the fundamental, while the 2β harmonic is unable to do so. The 2β harmonic could contribute to producing the subharmonic via interactions involving $3\beta/2$ or higher fractional harmonics such as $5\beta/2$. Of the higher frequencies capable of subharmonic production, the $3\beta/2$ is the most important because it also has the highest potential of extracting energy from the mean flow, considering that the 2β harmonic is already very nearly neutral when the fundamental experiences maximum amplification and all higher harmonics, fractional or not, are damped from their interaction with the mean flow. Indeed, as it will be demonstrated herein, if mode $3\beta/2$ is forced at a low level (lower than that of the naturally occurring fundamental) the production of the subharmonic can be considerably boosted. Similar forcing of the harmonic 2β by itself cannot achieve this.

In order to illustrate the effect of the three-wave interactions and the significance of the initial phase angles on the evolution of the modes as well as the mean flow, we have considered four sets of initial values θ_0 and φ_0 for the phase angle differences that control the binary and three-wave modal interactions, respectively. These four sets cover the cases where the initial binary interaction between the fundamental and the subharmonic is maximized simultaneously with the three-wave interaction between the subharmonic and mode $3\beta/2$. At the chosen initial fundamental frequency $\beta_0=0.44$, $\xi_{12}^1=38.4^\circ$, $\xi_{13}^2=165.3^\circ$, $\xi_{12}^3=29.4^\circ$, and $\xi_{23}^1=18.04^\circ$. Thus, the total interaction phase angles Ψ_{12}^1 and Ψ_{13}^2 are initially zero and the corresponding initial energy interactions are maximized in favor of the subharmonic [see Eq. (8)], when $\theta_0=-38.4^\circ$ and $\varphi_0=-165.3^\circ$. The same initial energy interactions are both strongly unfavorable to the subharmonic when $\theta_0=141.6^\circ$ and $\varphi_0=14.7^\circ$ rendering Ψ_{12}^1 and Ψ_{13}^2 initially equal to 180° . The total interaction phase angles Ψ_{12}^1 and Ψ_{13}^2 are initially 90° and the corre-

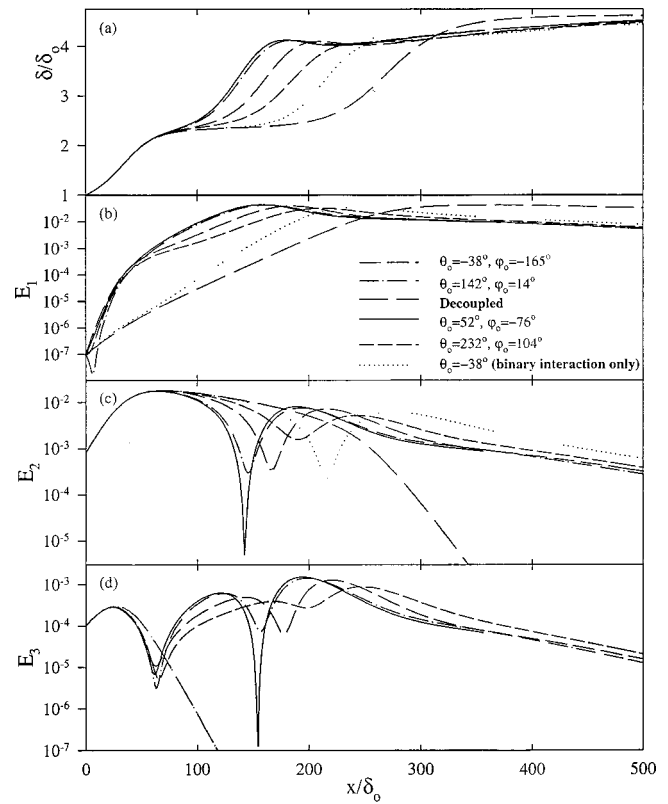


FIG. 1. Evolution of the shear layer thickness (a), the subharmonic (b), fundamental (c), and $3\beta/2$ (d) modal energies ($\beta_0=0.44$, $E_{10}=10^{-7}$, $E_{20}=8\times 10^{-4}$, $E_{30}=10^{-4}$).

sponding initial phase interactions are maximized causing a phase increase for all the modes [see Eq. (9)] when $\theta_0=51.6^\circ$ and $\varphi_0=-75.3^\circ$. These phase interactions are initially maximum but cause a decrease in modal phases when Ψ_{12}^1 and Ψ_{13}^2 are initially 270° for $\theta_0=231.6^\circ$ and $\varphi_0=104.7^\circ$. The initial levels of the three-wave interaction between the fundamental and subharmonic and the three-wave interaction between the fundamental and mode $3\beta/2$ are then dictated by the initial value of φ_0 for each of these four cases.

The calculated downstream development of the shear layer thickness and the three modal energies for the four cases described above is presented in Figs. 1(a)–1(d). The results of a calculation carried out with the three modes fully decoupled with each other, i.e., without including the wave interaction terms in the modal energy and phase equations, has been included as a baseline. Also included is a case where only the binary interaction between fundamental and subharmonic is activated and mode $3\beta/2$ is decoupled. The initial energies of the three modes have been chosen so that the fundamental is initially the strongest ($E_{20}=8\times 10^{-4}$), the subharmonic is weak ($E_{10}=10^{-7}$), and mode $3\beta/2$ ($E_{30}=10^{-4}$) is approximately an order of magnitude below the fundamental. Thus, in all cases the total large-scale structure energy content is constant. The magnitudes of these initial energies are comparable to those encountered in Ref. 10, and therefore realistic in terms of a forced experiment. On the basis of linear stability all three modes are initially in the amplification region, the fundamental starting out as the most

amplified one. Mode $3\beta/2$ begins its course on the right of the peak of the amplification-rate curve and looks forward to declining amplification rates and eventual dampening, while the subharmonic starts to the left of the peak and will experience maximum amplification when the fundamental is nearly neutral and mode $3\beta/2$ is dampened. In the decoupled case, the mode evolution is driven by their interaction with the mean flow. All modes are amplified by drawing energy from the mean flow and dampened as they return it to the mean flow. Mode $3\beta/2$, having the highest frequency, peaks first as it reaches neutral stability and monotonically decays thereafter [Fig. 1(d)]. The fundamental peaks further downstream [Fig. 1(c)] and is followed by the subharmonic [Fig. 1(b)]. The shear layer thickness, as shown for the decoupled case in Fig. 1(a) displays the familiar stepwise growth. The initial fast growth reflects the mean energy loss to the initially dominant fundamental mode while this is being amplified. The remaining two modes do not contribute significantly, being orders of magnitude weaker in this initial region. As the fundamental saturates and begins to decay by returning energy to the mean, the growth of the shear layer is almost brought to a halt. A weak growth is sustained primarily due to viscosity as well as the energy drawn by the growing subharmonic. As the latter becomes comparable in magnitude to the decaying fundamental, the energy drain of the mean flow by the growing subharmonic increases and fast growth of the shear layer is resumed until the subharmonic saturates and a second plateau of the shear layer thickness appears. The flow visualization done by Ref. 16, in conjunction with their measurements of shear layer thickness and modal energies, has indicated that the first rollover of the shear layer occurs in the neighborhood of the fundamental peak (first mean-thickness plateau), while “vortex pairing” is initiated when the subharmonic and fundamental share the same energy level and is completed near the subharmonic peaking location (second mean-thickness plateau). The dimensionless frequencies and local linear amplification rates of the three modes change with the thickness of the shear layer. Therefore, when the growth of the latter is slow, as in the plateaus displayed in Fig. 1(a), the amplification rates of the modes, dictated by the corresponding values of the mean and viscous integral coefficients in Eq. (8), also vary slowly. Thus the growth rate of the fundamental and subharmonic [Figs. 1(b) and 1(c)] in the region of the mean thickness plateau (within $100 < x/\delta_0 < 200$ approximately) remains nearly constant. These observations regarding the coupling between the evolution of noninteracting modes and the mean flow have been discussed in previous studies (e.g., Ref. 17) and have been repeated here because this coupling still forms the underlying basis of the flow and modal evolution in the presence of nonlinear modal interactions. This is partly evident from the fact that the stepwise growth of the shear layer created by the energy drain of the mean flow by the occasionally dominant mode, is a common feature of all cases presented in Fig. 1(a).

The results presented in Figs. 1(a)–1(d) for the four cases where all the nonlinear interactions between the three modes are present, are, overall, markedly different than both cases where only the binary interaction between fundamental

and subharmonic is active, and the fully decoupled one. The nonlinear, intramodal interactions leave the fundamental and mode $3\beta/2$ virtually unaffected during the early stages of their development and until they saturate [Figs. 1(c) and 1(d)]. Thus, the early growth rate of these two modes is adequately represented by that resulting from linear stability. The growth of the shear layer in the same region is similarly unaffected [Fig. 1(a)] because it is driven by the also unaffected fundamental. The subharmonic, however, being the weakest mode initially, is profoundly influenced by its nonlinear interactions with the other two modes. It is evident from Fig. 1(b) that the initial amplification rate of the subharmonic is substantially enhanced due to the interactions with the other modes. In the case where the two strongest interactions are initially unfavorable ($\theta_0 = 141.6^\circ$ and $\varphi_0 = 14.7^\circ$) the subharmonic is initially dampened because the combined energy drain from the higher frequency modes outpowers the gains from the mean flow. However, this situation is rather short-lived and the intramodal interactions quickly change to being strongly in favor of the subharmonic, which then resumes a much faster growth. It is also evident from the comparison with the pure binary interaction case in Fig. 1(b), that the three-mode interactions are responsible for the dramatic growth of the subharmonic in the early stages of its development while it is much weaker than the other two modes. Unlike the other two modes, the early growth of the subharmonic bears no resemblance to that predicted by linear stability. When the three-mode interactions are deactivated, the growth of the subharmonic, which is close to that indicated by linear stability, is markedly slower in this initial region. Compared to the effects of three-mode interactions, the binary interaction alone does not cause a dramatic departure of the early subharmonic growth rate from that indicated by linear stability. The accelerated growth of the subharmonic in the early stages of its development, resulting from the nonlinear interactions with both the other two modes, causes its peak to move considerably upstream from the location predicted by local linear stability (decoupled case) as well as the location predicted from the inclusion of binary interactions alone [Fig. 1(b)]. Thus the subharmonic becomes the dominant mode earlier and the shear layer resumes its fast growth after the saturation of the fundamental much sooner, as indicated in Fig. 1(a). The evolution of the fundamental and $3\beta/2$ modes is also strongly influenced by the nonlinear interactions downstream of their first peaks. The fundamental undergoes stronger dampening after passing through the neutral point, but experiences amplification again further downstream and reaches a second peak because of favorable intramodal interactions and in spite of the loss of energy to the mean flow. Mode $3\beta/2$ is similarly affected by means of three-mode interactions that contribute to its survival long after the drain of its energy by the mean flow begins. As a consequence it goes through a sequence of dampening followed by amplification resulting in two more peaks further downstream. These peaks caused purely by nonlinear interactions are stronger than the first one which is brought about by extraction of energy from the mean flow. Both the fundamental and the $3\beta/2$ modes survive downstream because of energy channeled to them from

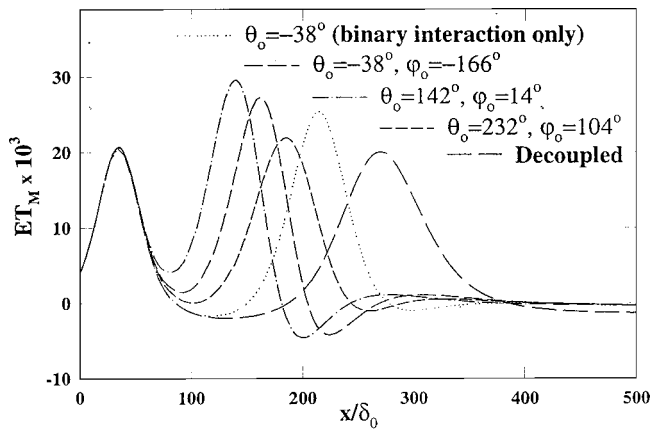


FIG. 2. Evolution of the net mean-flow interaction term ($\beta_0=0.44$, $E_{10}=10^{-7}$, $E_{20}=8 \times 10^{-4}$, $E_{30}=10^{-4}$).

the subharmonic through nonlinear interactions and resume a monotonic decay after the subharmonic begins its decline.

The comparison between the cases presented in Fig. 1 also shows the high sensitivity of the modal and mean flow evolution to the initial modal phases through the initial phase angle differences (θ_0 and φ_0) which control the initial strength and direction of both the energy and phase interactions. The early growth of the subharmonic and the location of its peak, the growth of the shear layer during subharmonic dominance, and the magnitude and locations of the secondary peaks of the two higher frequency modes, all display a strong dependence on the initial phase angles. It is noteworthy that the subharmonic peaks earlier, rising to a slightly higher level, in the case where its initial nonlinear interactions with the other modes are unfavorable ($\theta_0=141.6^\circ$; $\varphi_0=14.7^\circ$) rather than in the case where they are favorable ($\theta_0=-38.4^\circ$; $\varphi_0=-165.3^\circ$). This is a consequence of the nonlinear phase interactions which will be discussed later.

It is observed that, in three of the cases examined, the shear layer thickness is reduced after the subharmonic has saturated at the beginning of its second plateau. This behavior which has been observed in the experiments of Ref. 15 is due to the net return of energy to the mean flow by all three modes. This is evident in Fig. 2 where the net interaction term, $ET_M = \sum_1^3 (E_k I_{Mk})$ in Eq. (8), with the mean flow is given as a function of the downstream coordinate. The interaction is positive when energy is extracted from the mean flow and negative when it is returned. The two successive peaks of this term correspond to the peak growth of the shear layer during the dominance of the fundamental (first peak) and the subharmonic (second peak). Two of the three-mode cases shown in Fig. 2 display a pronounced negative peak after the second positive peak. The negative peak is a result of “negative production” causing the “negative growth” of the shear layer visible in Fig. 1(a). The sustained strength of mode $3\beta/2$, caused by three-mode, nonlinear interactions with the two lower frequencies while the former is returning energy to the mean, is primarily responsible for this negative growth of the shear layer. The fundamental which also sustains its strength through nonlinear modal interactions also contributes to the negative shear layer growth, but cannot

support it by itself as indicated by the absence of such behavior in the case where only binary interactions are allowed and mode $3\beta/2$ does not survive downstream. The negative peak of the mean interaction term far downstream is much weaker in this case (Fig. 2). The appearance of vigorous “negative production” after the saturation of the dominant mode (in this case the subharmonic) depends on the initial modal phase angles. One of the three-mode-interaction cases examined here ($\theta_0=231.6^\circ$; $\varphi_0=104.7^\circ$) does not display such behavior [Fig. 1(a)] the negative peak of the mean interaction term far downstream being weak (Fig. 2). Close inspection of Figs. 1(b)–1(d) reveals that the energy levels of both the fundamental and mode $3\beta/2$ when the subharmonic saturates are much lower in this case than in the other three cases where the “negative growth” of the shear layer is observed. The comparison between the cases shown in Fig. 2 also illustrates the profound indirect effect of the nonlinear interactions on the local transfer of energy between the mean flow and the large-scale structure, the latter represented by the three modes combined. The channeling of energy from the subharmonic to the higher frequency modes through nonlinear modal interactions (primarily three-mode ones) is the key to the appearance of the shear layer contraction, because the higher frequency modes are more effective in returning energy to the mean flow; the mean interaction integral, I_{Mn} , which is negative in the region past the neutral point, increases in magnitude with increasing frequency.¹⁷

The evolution of the four nonlinear modal interaction terms $[ET_{jk}^n = I_{jk}^n \sqrt{(E_1 E_2 E_3)/\delta}]$ in Eq. (8) is presented in Figs. 3(a)–3(d). The notation is such that when ET_{jk}^n is positive energy is transferred to mode j . Although the binary interaction between the subharmonic and fundamental is overall the strongest one throughout the domain of evolution, it is weak compared to the three-mode interactions in the early stages of development of the flow. This is evident from the details of the term evolution in the first few decades of initial thicknesses shown to the right of Figs. 3(a)–3(d). This relative weakness of the binary interaction is primarily due to the fact that the subharmonic is initially very weak and the ratio of the binary to the net three-mode interaction is proportional to $\sqrt{E_1/E_3}$. Thus, when the subharmonic is initially weak, the three-mode interactions are very significant in determining its initial growth. Comparison of the initial evolution of the binary interaction term (ET_{12}^1) in the absence of the three-mode interactions to that resulting when such interactions are present, shows that the binary interaction itself is strengthened as a result of the nonlinear coupling through these three-mode interactions. This leads to further enhancement of the initial subharmonic growth which consequently becomes able to draw more energy from the mean flow, thus compounding its growth. The result of this compound effect is the strikingly faster amplification of the subharmonic in the early stages of its development as shown in Fig. 1(b).

It is observed in Fig. 3 that each nonlinear, energy interaction term reverses direction several times in the course of the evolution of the flow. These reversals, which are often quite rapid, are shown later to be caused by the nonlinear variation of the modal phases (ψ_n) which influence the

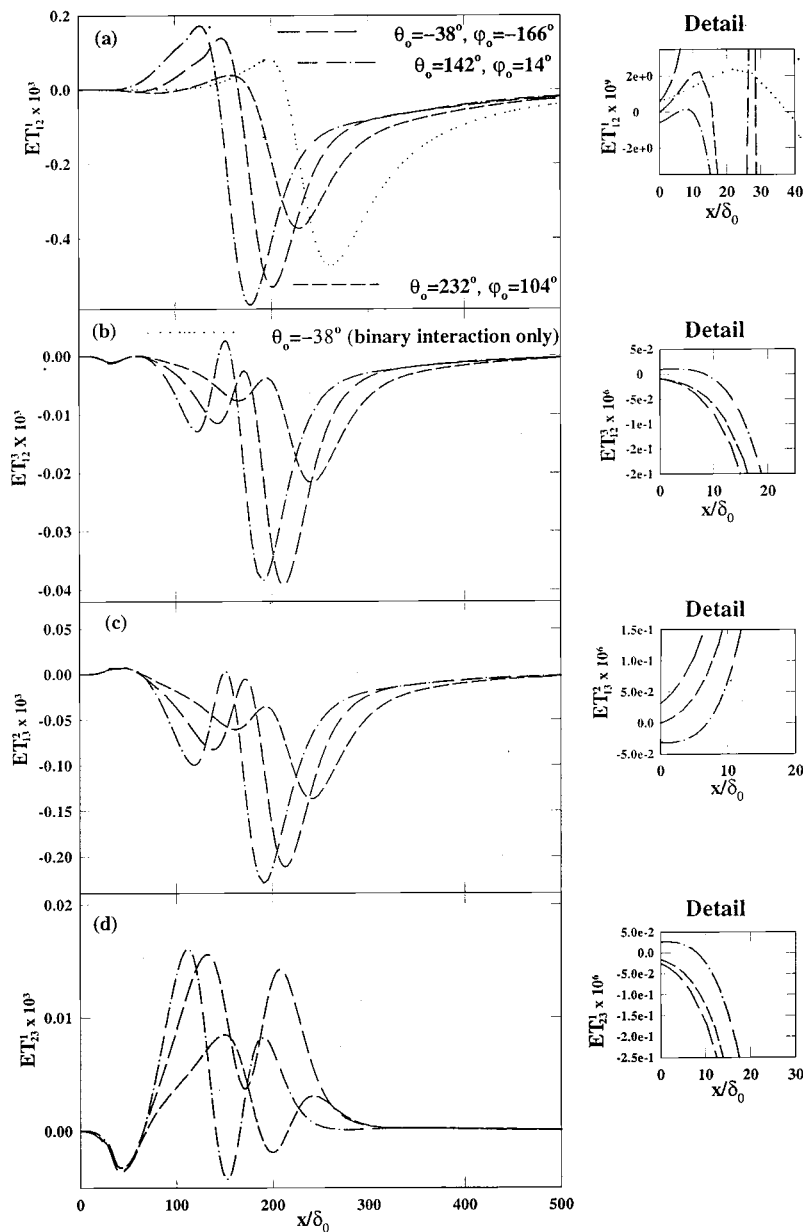


FIG. 3. Evolution of the nonlinear, intramodal interaction terms ($\beta_0=0.44$, $E_{10}=10^{-7}$, $E_{20}=8 \times 10^{-4}$, $E_{30}=10^{-4}$).

variation of the total interaction phase angles, Ψ_{jk}^n . The evolution of the latter is shown in Fig. 4. The positive and negative signs to the right of each figure indicate the ranges of the total interaction phase angles within which mode j gains or loses energy, respectively. Reversals of the energy interactions between modes are caused when the total interaction phase angles cross odd multiples of $\pi/2$. These reversals can be particularly violent if the corresponding total interaction phase angle experiences very rapid changes. For example, in the case where the initial interactions are strongly unfavorable to the subharmonic ($\theta_0=141.6^\circ$; $\phi_0=14.7^\circ$), the total interaction phase angle, Ψ_{12}^1 , of the binary interaction between the fundamental and the subharmonic shown in Fig. 4(a), decreases rapidly from its initial value of π , crossing into the first and fourth quadrants where the interaction becomes favorable to the subharmonic, then quickly continues into the third quadrant where the interaction turns once more against the subharmonic. This is visible in the detail of the

binary interaction term evolution, to the right of Fig. 3(a). This double reversal occurs within less than 20 initial thicknesses. The total interaction phase angle, Ψ_{13}^2 , controlling the interaction of the subharmonic with mode $3\beta/2$, displays similar behavior within the same, initial range of the streamwise coordinate. It decreases fast, from its initial value of π , into the first quadrant [Fig. 4(c)] and stabilizes to a near zero value before it undergoes another rapid change. As a result the corresponding interaction term shown in Fig. 3(c) (see detail) quickly reverses sign and becomes favorable to the subharmonic. Similar trends are observed in the evolution of the other two interactions and for every case examined.

Rapid variations of the total interaction phase angles have been measured by Ref. 27, using definitions similar to the ones used here, in their jet study. Apart from these rapid variations they also observed regions within the streamwise evolution where the total interaction phase angles remained constant, or nearly so. They identified these regions as ones

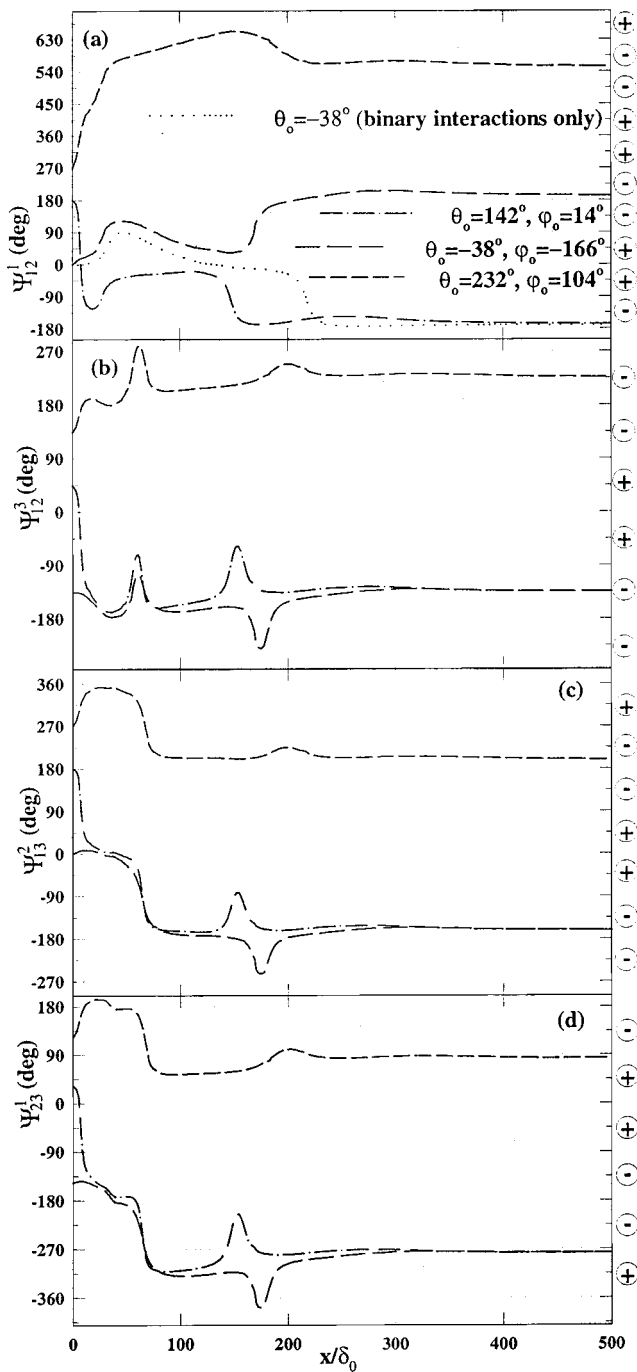


FIG. 4. Evolution of the total interaction phase angles ($\beta_0=0.44$, $E_{10}=10^{-7}$, $E_{20}=8 \times 10^{-4}$, $E_{30}=10^{-4}$).

of resonant interaction between the modes involved. Such regions of resonant interaction are also observed in our calculations as shown in Fig. 4. To be more precise a truly resonant energy interaction occurs when the corresponding total interaction phase angle is constant and equal to a multiple of π . This may not be possible in an exact sense, so we will accept the regions where this condition is approximately met as resonant ones. For instance, in the case where $\theta_0 = -38.4^\circ$ and $\varphi_0 = -165.3^\circ$, the binary interaction between fundamental and subharmonic is initially resonant in favor of the latter [Fig. 4(a)]. Resonant binary interaction also occurs in favor of the subharmonic further downstream between 100

and 200 initial thicknesses of the origin. Likewise, in the case where $\theta_0 = 141.6^\circ$ and $\varphi_0 = 14.7^\circ$, a near resonant binary interaction favoring the subharmonic is achieved between 30 and 130 initial thicknesses from the origin, while one favoring the fundamental is established from 160 thicknesses and so on. As a matter of fact, a resonant binary interaction in favor of the fundamental is established far downstream in all cases shown in Fig. 4(a). Three-mode resonant interactions are also present. For instance, in the case where $\theta_0 = 231.6^\circ$ and $\varphi_0 = 104.7^\circ$, all three-mode interactions are nearly resonant between approximately 10 and 50 initial thicknesses from the origin [see Figs. 4(b)–4(c)]. Also in both cases where $\theta_0 = -38.4^\circ$ and $\varphi_0 = -165.3^\circ$, and $\theta_0 = 141.6^\circ$ and $\varphi_0 = 14.7^\circ$, the three-mode interaction between the subharmonic and mode $3\beta/2$ becomes resonant favoring the subharmonic and then favoring mode $3\beta/2$ in quick succession within the first 150 thicknesses [see Fig. 4(c)]. As indicated in Fig. 3 the strongest peaks of the energy interaction terms appear in the regions where the resonance conditions are met. It is also observed that the three-mode resonant interactions are better defined and closer to the exact definition than the binary one. This is in support of Petersen and Clough's²⁷ argument that the three-mode resonance is the more dominant one.

As mentioned previously the rapid variations of the total interaction phase angles and the associated reversals in the nonlinear energy exchange between modes are caused by modal phase variations caused by nonlinear phase interactions. This is confirmed upon examination of the evolution of the net phase interaction terms for each mode in Eq. (9) defined as

$$PT_1 = \sqrt{\frac{E_2}{\delta}} P_{12}^1 + \sqrt{\frac{E_2 E_3}{\delta E_1}} (P_{13}^2 - P_{12}^3), \quad (12)$$

$$PT_2 = \frac{E_1}{\sqrt{E_2} \delta} P_{12}^1 + \sqrt{\frac{E_1 E_3}{\delta E_2}} (P_{12}^3 - P_{23}^1), \quad (13)$$

$$PT_3 = \sqrt{\frac{E_1 E_2}{\delta E_3}} (P_{13}^2 + P_{23}^1), \quad (14)$$

and presented in Fig. 5. The net phase interactions become very significant over narrow bands of the stream wise coordinate causing rapid local variations of the modal phases (ψ_n) which in turn result in rapid variations of the total interaction phase angles. This is evident from the fact that the streamwise locations in Fig. 4, where the total interaction phase angles experience rapid variation, coincide with the locations of peak net phase interaction. For instance, in the case where the subharmonic is dampened due to initial unfavorable interactions with the other modes ($\theta_0 = 141.6^\circ$; $\varphi_0 = 14.7^\circ$) the rapid reduction of all the total interaction phase angles in Fig. 4, is due to the strong increase in the subharmonic phase, ψ_1 , caused by a strong nonlinear phase interaction as shown by the peak of PT_1 near the origin of the streamwise coordinate in Fig. 5(a). Similarly, the sharp decreases in the three-mode, total interaction phase angles around 65 initial thicknesses from the origin, for both cases with $\theta_0 = -38.4^\circ$ and $\varphi_0 = -165.3^\circ$, and $\theta_0 = 141.6^\circ$ and

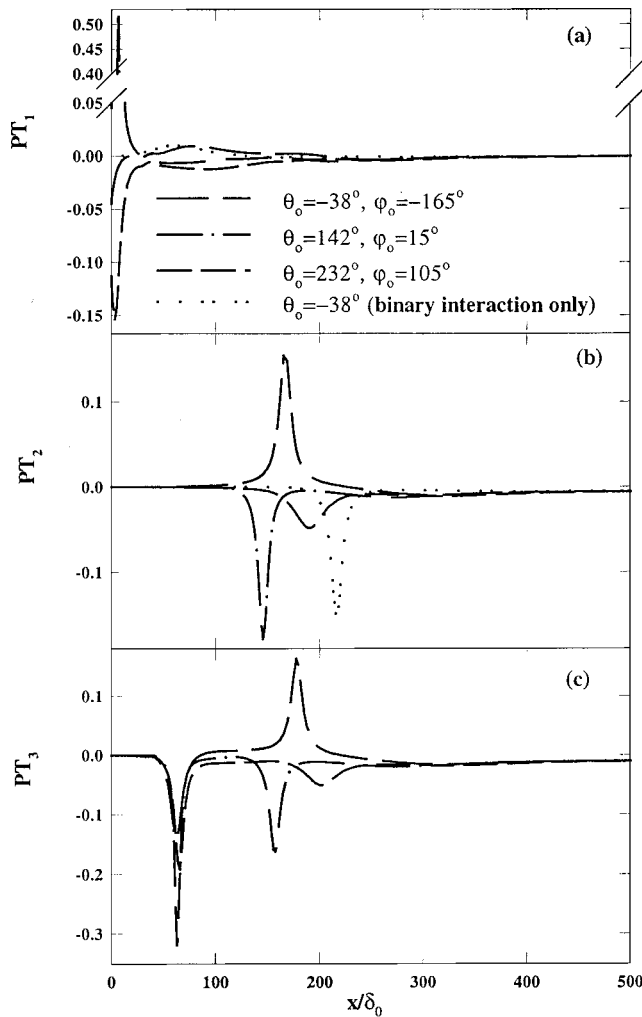


FIG. 5. Evolution of net modal phase interaction terms ($\beta_0 = 0.44$, $E_{10} = 10^{-7}$, $E_{20} = 8 \times 10^{-4}$, $E_{30} = 10^{-4}$).

$\varphi_0 = 14.7^\circ$ in Figs. 4(b)–4(d), coincide in location with the decrease in the phase of mode $3\beta/2$, ψ_3 , caused by the strong nonlinear phase interaction indicated by the peak of PT_3 in Fig. 5(c). Apart from the strong peaks (positive or negative) of the phase interaction terms there are weaker ones caused by the maxima of modal energy densities found in the numerators of these terms and/or by extrema of the interaction coefficients when the total interaction phase angles approach odd multiples of $\pi/2$. Reversal in the direction of the modal phase interactions occur when the total interaction phase angles cross multiples of π .

The regions of strong nonlinear phase interactions are associated with the regions where the corresponding modal energy is weak, through the square root of the modal energy density in the denominator of the interaction terms as shown in Eqs. (12)–(14), and as discussed in a previous section. This is also obvious from a comparison of the locations where peaks of the net modal phase interactions appear in Fig. 5, to the locations of the corresponding minima in the modal energy evolution of Fig. 1. The localized strong coupling of the modal phase variation with that of the modal energy density is responsible for the rapid reversal of nonlinear energy interactions in favor of the occasionally declin-

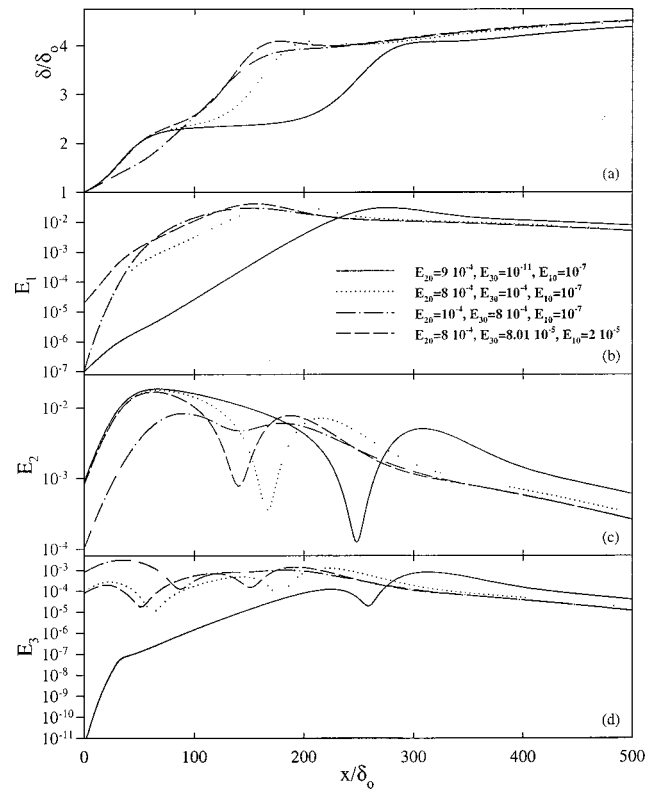


FIG. 6. Initial modal energy effect: shear layer thickness (a), subharmonic (b), fundamental (c), and mode $3\beta/2$ (d) energies ($\beta_0 = 0.44$, $\theta_0 = -38^\circ$, $\varphi_0 = -165^\circ$).

ing mode. Thus, a nonlinear mechanism is identified that preserves the higher frequency modes far downstream by channeling energy to them from stronger, lower frequencies whenever the former are considerably weakened. In a more general sense this mechanism is activated whenever any of the modes is weakened. The results of this mechanism are evident in the evolution of the fundamental and $3\beta/2$ modes far downstream in Figs. 1(a) and 1(b), as well as in the rapid recovery of the declining subharmonic in the case where the interactions with the other modes are initially adverse [case with $\theta_0 = 141.6^\circ$ and $\varphi_0 = 14.7^\circ$ in Fig. 1(b)].

In the cases examined thus far we have held the initial modal energy contents constant while varying the initial modal phase angles. The evolution of the modes and modal interactions, as well as the evolution of the flow, is also dependent on the initial modal energies.^{17,41} The effects of the variation of the initial modal energies are shown in Fig. 6, where the shear layer growth and the modal energy evolution are presented for four different initial modal energy combinations. In all cases the total large-scale energy is constant ($E_{10} + E_{20} + E_{30} = 9.01 \times 10^{-4}$) and the initial phase angle differences are set to $\theta_0 = -38.4^\circ$ and $\varphi_0 = -165.3^\circ$. The importance of the three-wave interaction effect on the development of the subharmonic is immediately evident from the results of the case where mode $3\beta/2$ is initially extremely weak ($E_{30} = 10^{-11}$). The initial weakness of this mode trivializes the effect of the three-mode interactions on the amplification rate of the subharmonic in the initial region and thus the subharmonic undergoes slower growth [Fig.

6(b)]. Because of the slower initial amplification of the subharmonic in this case, its peak is moved downstream as is the second fast growth of the shear layer during its dominance. Contrary to the other two initially stronger modes, mode $3\beta/2$ is profoundly influenced by the interaction with them. It is seen in Fig. 6(d) that its growth is sustained far downstream, even while it returns energy to the mean flow, and it reaches its highest peak at a location downstream of the highest peaks of both the subharmonic and the fundamental. This behavior, as we have seen before, is characteristic of the combined nonlinear energy and phase interactions which consistently favor the weaker modes at the expense of the stronger ones, independently of the frequency. This is also indicated by the slower initial growth of the subharmonic when its initial strength is larger (case with $E_{10}=2\times 10^{-5}$) as opposed to the faster initial growth it experiences when it is initially two orders of magnitude weaker (cases where the subharmonic is initially the weakest mode with $E_{10}=10^{-7}$). Although the three-mode interactions have a lesser effect on the subharmonic when this is initially stronger, the more vigorous interaction with the mean flow contributes to its higher and earlier energy peak in Fig. 6(b), accompanied by earlier accelerated growth of the shear layer in Fig. 6(a). In the case where mode $3\beta/2$ is initially forced at a level that makes it dominant ($E_{30}=8\times 10^{-4}$) the initial fast growth of the shear layer is suppressed [Fig. 6(a)] because of the relatively weaker fundamental. The subharmonic, being the weakest mode, experiences the rapid growth generated by three-mode interactions and quickly overtakes both the fundamental and mode $3\beta/2$. Consequently, as seen in Fig. 6(a), the subharmonic immediately becomes the only factor responsible for the fast growth of the shear layer. Contraction of the shear layer, associated with the compound effect of the energy returned to the mean by all three modes, is observed in the region immediately downstream of the subharmonic peak in two of the cases examined and is fueled by the simultaneous strong peaks of the other two modes. In the remaining two cases the growth of the shear layer is reduced but not reversed in the corresponding region.

As seen in Fig. 6, in the case where mode $3\beta/2$ and/or higher frequencies are initially weak, binary interactions alone could be primarily responsible in determining the evolution of the flow. Such a case is also depicted in Fig. 7, where the results from the present method are compared with mode II from the experiments of Ref. 10. The subharmonic which was forced in this experiment was sufficiently strong initially while higher frequencies were weak. Therefore only binary interaction is presumed to be significant. The initial phase angles were not measured during the experiments, so the initial phase angle difference used for the calculations was arbitrarily set to $\theta_0=170^\circ$. The agreement with the experiments is qualitatively good. The growth of the shear layer is reasonably well predicted in the region of fundamental and subharmonic dominance until far downstream where small-scale turbulence dictates the growth [Fig. 7(a)]. The location of the fundamental and subharmonic peaks in Fig. 7(b) are also well predicted as well as the survival of the fundamental far downstream with the appearance of a local minimum in its energy, although this is more pronounced in

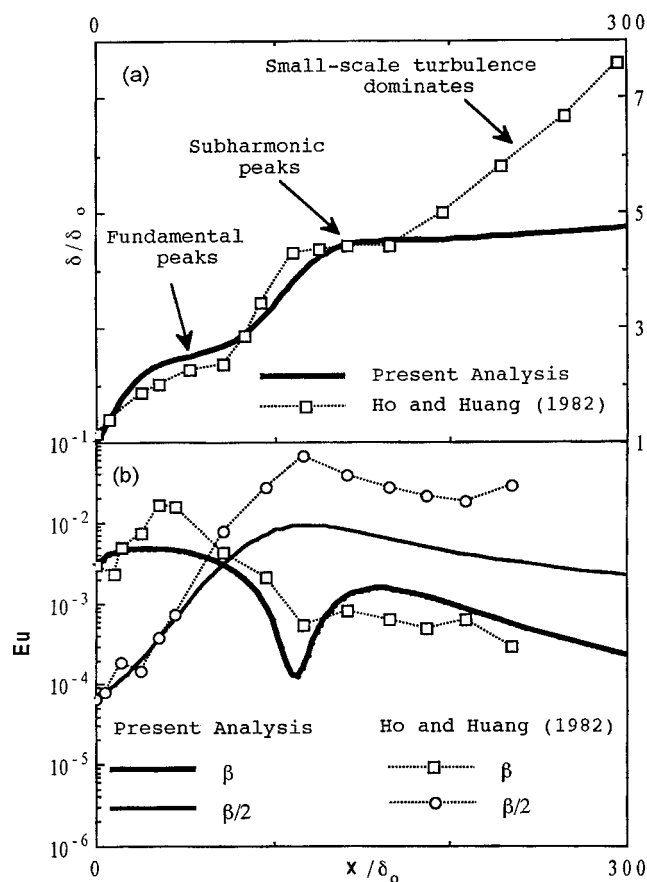


FIG. 7. Mean-flow (a) and modal energy (b) evolution of a shear layer perturbed by forcing the first subharmonic. Comparison with mode II from Ho and Huang's (Ref. 10) experiments ($\beta_0=0.51$, $\theta_0=170^\circ$).

the calculation than it is in the experiment. The results from the present analysis taking into account the nonlinear variation of the phases show improvement over those obtained by Ref. 17, where the variation of the phases was assumed to be that dictated by linear analysis. The collective effect of the presence of other modes, although individually weak, in the experiments as well as that of the small-scale turbulence certainly contribute to the quantitative differences between the calculated and measured quantities.

From a practical standpoint the results shown in Fig. 6 indicate that the subharmonic can be indirectly boosted to cause faster and earlier growth of the shear layer through vortex merging, by forcing mode $3\beta/2$ rather than, or in addition to, the subharmonic itself. Thus a two-frequency forcing scheme can be used to enhance large-scale induced mixing in the shear layer. The key mechanism that makes such a manipulation of the shear layer successful is that introduced by nonlinear three mode interactions.

B. Interactions involving mode $2\beta/3$

Another situation where three-mode interactions are likely to be of considerable importance is one where the second subharmonic ($\beta/3$) of the fundamental most amplified frequency (β) is forced. Such is the case of mode III in the experiments of Ref. 10. Their measurements indicate a strong presence of a $2\beta/3$ mode which can interact through

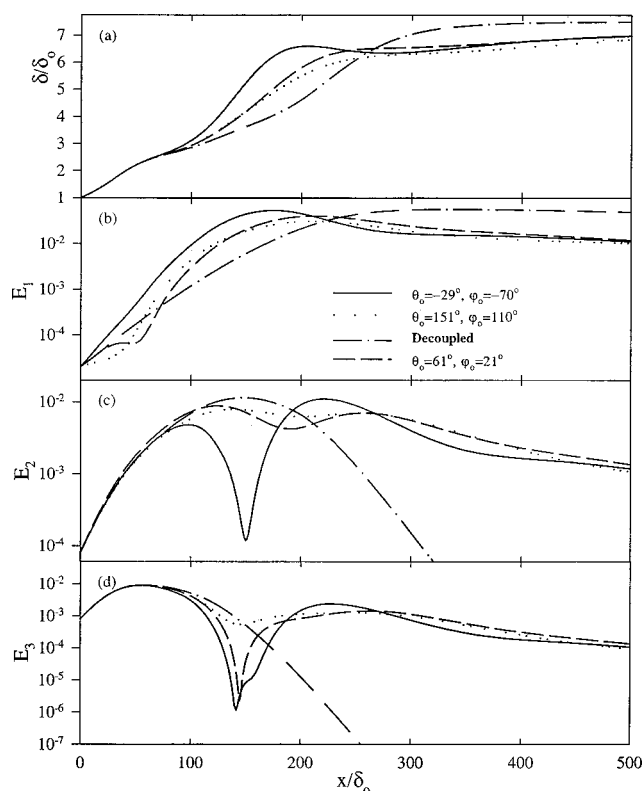


FIG. 8. Evolution of the shear layer thickness (a), the second subharmonic (b), mode $2\beta/3$ (c), and fundamental (d) modal energies ($\beta_0 = 0.44$, $E_{10} = 2 \times 10^{-5}$, $E_{20} = 8.01 \times 10^{-5}$, $E_{30} = 8 \times 10^{-4}$).

binary and three-mode interactions with the second subharmonic, while acting as an energy broker in the three-mode interaction of the second subharmonic with the fundamental. This indirect interaction between the fundamental and second subharmonic is the only one possible, if higher frequency modes are weak or absent. It is also likely that this interaction is the strongest one overall, even if other three-mode interactions linking the subharmonic and fundamental modes are present through the participation of higher frequencies (e.g., $4\beta/3$). This is expected because of the higher potential for amplification possessed by the $2\beta/3$ mode in contrast to higher frequencies.

Solutions to this three-mode interaction problem were obtained using initial frequencies $\beta_0/3$, $2\beta_0/3$, and β_0 for the three modes, where the frequency of the fundamental β_0 is again approximately equal to β_m . Results of the calculation are shown in Fig. 8 for three initial phase difference combinations and the decoupled case as reference. The initial binary interaction of the second subharmonic with mode $2\beta/3$, and the three-mode interaction of the former with the fundamental are initially maximized when $\theta_0 = -29^\circ$ and $\varphi_0 = -70^\circ$, minimized when $\theta_0 = 151^\circ$ and $\varphi_0 = 110^\circ$, and nullified when $\theta_0 = 61^\circ$ and $\varphi_0 = 81^\circ$. In the last case the corresponding initial phase interactions are maximized. The initial energy levels of the three participating modes are held constant so that the fundamental is the strongest mode and the second subharmonic the weakest at the onset. The growth of the shear layer displays the same general trend with two regions of fast growth and two plateaus corresponding to the

dominance and saturation of the fundamental and the second subharmonic, respectively. The level of the second plateau is between 6 and 7 units depending on the case, which is roughly three times that of the first (between 2 and 2.5 units) as also observed by Ref. 10. The same general trends observed in the previous three-mode interaction case are present here as well, and the sensitivity of the modal and mean flow development to the initial phases is also evident in the results of Fig. 8. The second subharmonic, being initially the weakest mode is strongly affected by the nonlinear modal interactions, particularly during the early stages of its development. The other two modes are sustained far downstream, while returning energy to the mean flow, by extracting energy from the stronger second subharmonic. The same nonlinear mechanism, discussed previously, that causes rapid phase shifts of the weaker and declining modes until their energy interaction with other stronger modes becomes favorable, is in effect here as well. This is evident from the fast recovery of the second subharmonic from initially unfavorable modal interactions in Fig. 8(b), as well as the revival of the higher frequency modes far downstream [Figs. 8(c) and 8(d)]. It is also noteworthy that, in one of the cases presented, the highest energy peak of mode $2\beta/3$ occurs well after it has begun returning energy to the mean flow. This behavior is exclusively due to nonlinear interactions. Examination of the individual interaction terms, which are not shown here, indicates that three-mode interactions are of paramount importance for this mode combination as well as that presented in the previous section. The early growth of the initially dominant fundamental mode is unaffected by the nonlinear interactions in the region of its dominance and is primarily governed by the interaction with the mean flow. This is indicated from the comparison of the three-mode interaction solutions with the decoupled case in Fig. 8(d). On the basis of the same comparison, mode $2\beta/3$ is only weakly affected by the nonlinear interactions initially, slightly departing from the growth pattern dictated by its interaction with the mean. It is also interesting to observe that the contraction of the shear layer, observed downstream of the subharmonic peak in the previously examined subharmonic-fundamental-mode $3\beta/2$ interaction case, is also present here [$\theta_0 = -29^\circ$ and $\varphi_0 = -70^\circ$ in Fig. 8(a)]. It is thus apparent that this behavior is not exclusively a consequence of the action of frequencies higher than the most amplified fundamental (e.g., harmonics), although it occurs when the dimensionless frequency of the subharmonic is past the neutral value. The contraction appears in the region where strong second peaks of the fundamental and mode $2\beta/3$ coincide, and the net return of energy to the mean overpowers the viscous growth. We should point out, that in a turbulent shear layer the contraction of the thickness may not appear due to the action of small scale turbulence. Another possible cause of the shear layer contraction may be the distortion of the mean flow profile because of strong large-scale structure forcing. This effect has not been considered here, the shape of the mean flow profile having been assumed fixed. Nevertheless, the mechanism for mean flow contraction discussed above is in place and is indirectly driven by large-scale multimode interactions.

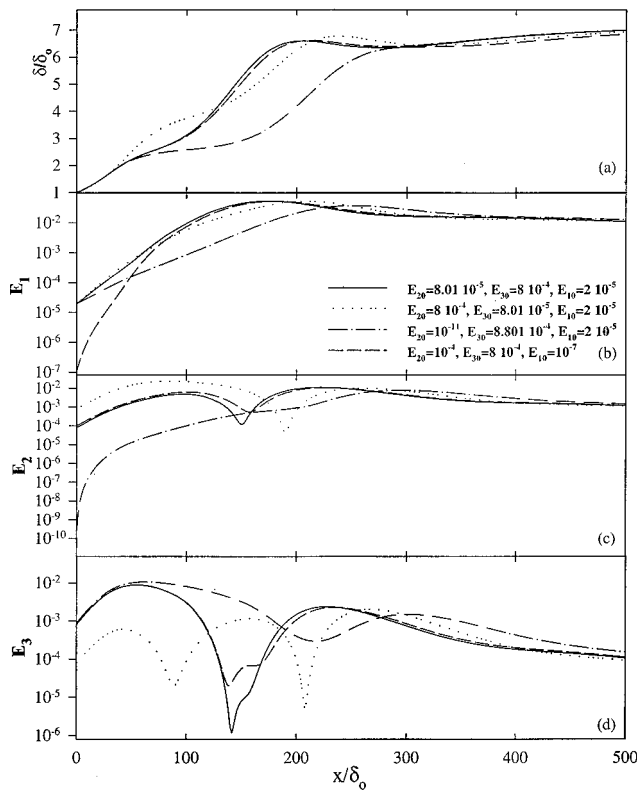


FIG. 9. Initial modal energy effect: shear layer thickness (a), second subharmonic (b), mode $2\beta/3$ (c), and fundamental (d) energies ($\beta_0=0.44$, $\theta_0=-29^\circ$, $\varphi_0=-70^\circ$).

As expected the modal evolution and flow development is sensitive to the initial energy content of the modes in this case as well. The results from four different combinations of initial energies at constant initial phase differences ($\theta_0=-29^\circ$ and $\varphi_0=-70^\circ$) are shown in Fig. 9. The significant effect of mode $2\beta/3$ on the early development of the second subharmonic and the downstream growth of the shear layer is most evident by the drastic reduction of the early growth of the second subharmonic and the shifting of its peak far downstream [Fig. 9(b)] when the initial energy of mode $2\beta/3$ is reduced (case with $E_{20}=10^{-11}$). As a consequence the first plateau of the shear layer is more pronounced and the fast growth caused during the dominance of the subharmonic is also moved downstream [Fig. 9(a)]. The early growth of mode $2\beta/3$ in this case is extremely fast and its peak energy appears at a location which is much further downstream than that expected from linear stability considerations. It is therefore evident that the evolution of this mode is dictated predominantly by nonlinear interactions with the other modes. When mode $2\beta/3$ is forced to be initially dominant (case with $E_{20}=8.01\times 10^{-4}$) the associated fast growth of the shear layer is more pronounced and the first plateau is moved to a higher level. This is expected because of the longer amplification history of this mode from its interaction with the mean flow.

A comparison of results from the present analysis with mode III from the experiments of Ref. 10 is presented in Fig. 10. The shear layer was forced by the second subharmonic of the most amplified frequency in the experiments and mode

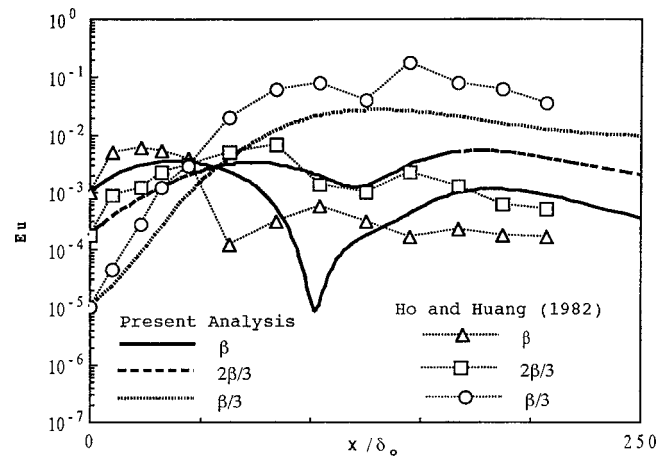


FIG. 10. Modal energy evolution in a shear layer perturbed by forcing the second subharmonic. Comparison with mode III from Ho and Huang's (Ref. 10) experiments ($\beta_0=0.51$, $\theta_0=170^\circ$, $\varphi_0=220^\circ$).

$2\beta/3$, although not forced, was observed in considerable strength while much weaker fractional and integer harmonics also appeared in the spectra. Thus, the three mode interaction problem was solved with the second subharmonic, the fundamental and mode $2\beta/3$ as the participating modes, ignoring higher frequencies and the small-scale turbulence which was initially weak in the experiments. The initial phase angles for the three modes were not measured during the experiment. The solution presented in Fig. 10 was obtained with $\theta_0=170^\circ$ and $\varphi_0=220^\circ$ as the initial phase angle differences. All the qualitative features of the modal energy evolution are present both in the experiment and the calculation. The survival of the two higher frequencies long after they have stopped gaining energy from the mean flow, the local energy minima and the secondary peaks of their energies far downstream as they appear in the experiments attest to the action of the intramodal, nonlinear energy interactions. The recovery of the higher modes leading to the secondary peaks also implies intramodal energy interaction reversals which are tied to the nonlinear evolution of the modal phases as discussed previously. The good qualitative agreement between the experiment and the calculation indicates that the three-frequency model used here is adequate in representing the most significant features of the large-scale structure and mean-flow evolution. However, inclusion of some of the relevant harmonics (e.g., $4\beta/3$, $5\beta/3$, and 2β), which will introduce additional intramodal binary and three-mode interaction channels, as well as small-scale turbulence could improve the quantitative agreement.

IV. CONCLUSIONS

A formulation based on the integral energy method has been presented for the nonlinear interaction problem between three large-scale coherent modes in a developing, laminar, free shear layer. Both binary and three-mode nonlinear interactions were included. Intramodal interactions have direct and indirect effects on the evolution of the flow. While the direct effect is weak, the indirect one is of particular importance because it involves a booster mechanism for energy

exchanges with the mean flow. The analysis accounts for the nonlinear variation of both the modal energies and phases. The two specific cases examined and discussed here are relevant to situations arising when the first and second subharmonic of the most amplified frequency (fundamental) are, respectively, forced and the initial small-scale turbulence level in the shear layer is weak. When the first subharmonic is forced the 3/2 harmonic of the fundamental is shown to play a significant role in the mean flow and modal evolution through three-mode interactions. Depending on the initial energy contents of the participating modes, these three-mode interactions can be of higher significance than the binary ones. Thus, our results support the argument of Ref. 27 according to which the associated three-mode resonances may be more dominant than the binary ones. The same conclusion can be reached regarding three-mode interactions involving a mode with frequency at 2/3 of the fundamental in the case where the second subharmonic of the latter is forced. The nonlinear interaction problem, the modal evolution, and the development of the mean flow are very sensitive to the initial energy contents and phases of the participating modes. Modes that are initially dominant are essentially unaffected by nonlinear interactions and experience growth at rates primarily dictated by their direct interaction with the mean flow and corresponding to those dictated by linear analysis. The occasionally weaker modes are profoundly effected by nonlinear interactions with stronger ones.

Reversals in the nonlinear energy exchange between modes are shown to be caused by rapid modal phase variations resulting from nonlinear phase interactions. These nonlinear phase interactions increase in strength when one or more of the participating modes is substantially weakened. Therefore, a strong coupling of the modal phase variations with the variations of the modal energies exists and is responsible for the rapid reversal of the nonlinear, intramodal energy interactions in favor of the occasionally declining mode. This nonlinear mechanism preserves the higher frequency modes far downstream by channeling energy to them from stronger, lower frequencies whenever the former are considerably weakened. As a result, higher frequencies that are initially weaker tend to peak much further downstream from the location expected from their interaction with the mean flow alone and predicted by linear analysis. In general, this mechanism is shown to be activated whenever any of the modes is weakened independently of its frequency. The preservation of the higher frequencies, by virtue of this nonlinear mechanism, while they are returning energy to the mean flow far downstream, is shown to contribute indirectly to the appearance of mean flow contraction. Mean flow contraction, which has been observed in experiments,¹⁵ is evidenced in this study when all three participating modes are returning energy to the mean flow far downstream and only in cases where the higher frequency modes were simultaneously strong as a result of three-mode nonlinear interactions. It should be noted, that in a turbulent shear layer, the contraction of the mean flow may not always appear due to the action of small scale turbulence. An other contributing factor to the shear layer contraction may be the distortion of the mean flow profile because of strong large-scale structure

forcing. This effect has not been considered here, the shape of the mean flow profile having been assumed fixed. Nevertheless, the mechanism for mean flow contraction discussed above is in place and is indirectly driven by large-scale multimode interactions.

Despite the fact that small-scale turbulence effects as well as the presence of additional modes (primarily higher harmonics) have been neglected in the present analysis, our results are in good qualitative agreement with the experiments of Ref. 10. From a practical standpoint our results also indicate that subharmonics can be boosted indirectly to cause faster growth of the shear layer through vortex merging, by forcing higher frequencies, which satisfy the three-mode, frequency-resonance condition, rather than, or in addition to, forcing the subharmonic itself. Thus a two-frequency forcing scheme can be employed to enhance large-scale induced mixing in the shear layer. The key mechanism that can make such manipulation of the flow successful is that introduced by nonlinear three mode interactions, their effect being dependent on the initial amplitudes and phases of the large-scale modes involved.

ACKNOWLEDGMENTS

This work was initiated through support by the Fluid Dynamics Program of the Office of Naval Research at the Division of Engineering, Brown University. It has been partially supported by the Louisiana State University Council on Research, the Louisiana Board of Regents, NASA EPSCoR through Grant No. NCCW-0059, NASA/Lewis Research Center through Grant No. NAG3-1016, and by the National Science Foundation through Grant No. MSM83-20307.

APPENDIX: INTEGRAL COEFFICIENTS: MEAN FLOW

$$\begin{aligned}
 I_M &= -\frac{1}{2} \int_{-\infty}^0 u^0(\eta) \{u^0(\eta)^2 - (1+R^2)\} d\eta \\
 &\quad - \frac{1}{2} \int_0^{+\infty} u^0(\eta) \{u^0(\eta)^2 - (1-R^2)\} d\eta \\
 &= 2R^2(1.5 - \ln 2), \\
 I_D &= R^2 \int_{-\infty}^{+\infty} \text{sech}^4 \eta d\eta = \frac{4R^2}{3}, \\
 W_{Mn} &= 2R \int_{-\infty}^{+\infty} \text{sech}^2 \eta \{ \alpha_n \phi_n \phi_n^{*'} \} d\eta, \\
 I_{Mn} &= \Im(W_{Mn}); \quad P_{Mn} = \Re(W_{Mn}), \\
 I_{Dn} &= 2 \left\{ |\alpha_n|^2 + \int_{-\infty}^{+\infty} \{ |\phi_n''|^2 + |\alpha_n \phi_n'|^2 \} \right\}, \\
 P_{Dn} &= 4 \Im(\alpha_n) \Re(\alpha_n), \\
 I_n &= 1 - R \int_{-\infty}^{+\infty} \tanh \eta \{ |\phi_n'|^2 + |\alpha_n \phi_n|^2 \} d\eta,
 \end{aligned}$$

$$S_{11}D_2 = 2e^{i(\psi_2 - 2\psi_1)} \int_{-\infty}^{+\infty} i(\alpha_2^* [\phi_2^{*'} \{\phi_1'^2 + \alpha_1^2 \phi_1^2\} \\ + \alpha_1 \phi_1 \phi_1' \alpha_2^* \phi_2^{*'}] + \alpha_1 \phi_1 \phi_1' \phi_2^{*'}) d\eta,$$

$$S_{21}D_3 = 2e^{i(\psi_3 - \psi_2 - \psi_1)} \int_{-\infty}^{+\infty} i(\alpha_3^* \phi_3^{*'} \{\phi_1' \phi_2' \\ + \alpha_1 \phi_1 \alpha_2 \phi_2\} + \alpha_1 \phi_1 \phi_2' \alpha_3^{*2} \phi_3^{*'} \\ + \alpha_2 \phi_2 \phi_1' \phi_3^{*'}) d\eta,$$

$$S_{12}D_3 = 2e^{i(\psi_3 - \psi_2 - \psi_1)} \int_{-\infty}^{+\infty} i(\alpha_3^* \phi_3^{*'} \{\phi_1' \phi_2' \\ + \alpha_1 \phi_1 \alpha_2 \phi_2\} + \alpha_2 \phi_2 \phi_1' \alpha_3^{*2} \phi_3^{*'} \\ + \alpha_1 \phi_1 \phi_2' \phi_3^{*'}) d\eta,$$

$$S_{31}D_2 = 2e^{i(\psi_3 - \psi_2 - \psi_1)} \int_{-\infty}^{+\infty} i(\alpha_2 \phi_2' \{\alpha_1 \phi_1 \alpha_3^* \phi_3^{*'} \\ - \phi_1' \phi_3^{*'}\} + \alpha_1 \phi_1 \phi_2 \alpha_2^2 \phi_3^{*'} - \alpha_3^* \phi_3^* \phi_1' \phi_2'') d\eta.$$

- ¹G. L. Brown and A. Roshko, "On density effects and large structure in turbulent mixing layers," *J. Fluid Mech.* **64**, 775 (1974).
- ²C. D. Winant and F. K. Browand, "Vortex pairing, the mechanism of turbulent mixing-layer growth at moderate Reynolds number," *J. Fluid Mech.* **63**, 237 (1974).
- ³H. W. Liepmann, "Free turbulent flows," in *Mécanique de la Turbulence* (CNRS, Paris, 1962), pp. 211–227.
- ⁴J. T. C. Liu, "Contributions to the understanding of coherent structures in free turbulent shear flows," *Adv. Appl. Mech.* **26**, 183 (1988).
- ⁵J. T. Stuart, "Nonlinear stability theory," *Annu. Rev. Fluid Mech.* **3**, 347 (1971).
- ⁶M. Gaster, E. Kit, and I. Wygnanski, "Large-scale structures in a forced turbulent mixing layer," *J. Fluid Mech.* **150**, 23 (1985).
- ⁷J. T. C. Liu, "Coherent structures in transitional and turbulent free shear flows," *Annu. Rev. Fluid Mech.* **21**, 285 (1989).
- ⁸C. M. Ho and P. Huerre, "Perturbed free shear layers," *Annu. Rev. Fluid Mech.* **16**, 365 (1984).
- ⁹P. A. Monkewitz and P. Huerre, "Influence of the velocity ratio on the spatial instability of mixing layers," *Phys. Fluids* **25**, 1137 (1982).
- ¹⁰C. M. Ho and L. S. Huang, "Subharmonics and vortex merging in mixing layers," *J. Fluid Mech.* **119**, 443 (1982).
- ¹¹I. Wygnanski and I. Weisbrot, "On the pairing process in an excited planar turbulent mixing layer," *J. Fluid Mech.* **195**, 161 (1988).
- ¹²Y. Q. Zhang, C. M. Ho, and P. A. Monkewitz, "The mixing layer forced by fundamental and subharmonic," in *Laminar-Turbulent Transition*, IUTAM Symposium, Novosibirsk, edited by V. V. Kozlov (Springer, Berlin, 1985), pp. 385–395.
- ¹³H. E. Fiedler and P. Mensing, "The plane turbulent shear layer with periodic excitation," *J. Fluid Mech.* **150**, 281 (1985).
- ¹⁴B. Dziomba and H. E. Fiedler, "Effect of initial conditions on two-dimensional free shear layers," *J. Fluid Mech.* **152**, 419 (1985).
- ¹⁵I. Weisbrot and I. Wygnanski, "On coherent structures in a highly excited mixing layer," *J. Fluid Mech.* **195**, 137 (1988).
- ¹⁶D. E. Nikitopoulos and J. T. C. Liu, "Triple-mode interactions in a developing shear layer," *Bull. Am. Phys. Soc.* **29**, 1548 (1984).
- ¹⁷D. E. Nikitopoulos and J. T. C. Liu, "Nonlinear binary-mode interactions in a developing mixing layer," *J. Fluid Mech.* **179**, 385 (1987).
- ¹⁸D. E. Nikitopoulos and J. T. C. Liu, "Nonlinear coherent mode interactions and the control of shear layers," in *Structure of Turbulence and Drag Reduction*, IUTAM Symposium Zürich/Switzerland, edited by A. Gyr (1990), pp. 119–127.
- ¹⁹R. R. Mankbadi, "On the interaction between fundamental and subharmonic instability waves in a turbulent round jet," *Phys. Fluids A* **3**, 595 (1991).
- ²⁰R. R. Mankbadi, "Dynamics and control of coherent structures in turbulent jets," *Adv. Appl. Mech.* **45**, 219 (1992).
- ²¹M. R. Hajj, R. W. Miksad, and E. J. Powers, "Subharmonic growth by parametric resonance," *J. Fluid Mech.* **236**, 35 (1992).
- ²²P. C. Patnaik, F. S. Sherman, and G. M. Corcos, "A numerical simulation of Kelvin–Helmholtz waves of finite amplitude," *J. Fluid Mech.* **73**, 215 (1976).
- ²³J. J. Riley and R. W. Metcalfe, AIAA Paper No. 80-0274, 1980.
- ²⁴R. E. Kelly, "On the stability of an inviscid shear layer which is periodic in space and time," *J. Fluid Mech.* **27**, 657 (1967).
- ²⁵P. A. Monkewitz, "Subharmonic resonance, pairing, and shredding in the mixing layer," *J. Fluid Mech.* **188**, 223 (1988).
- ²⁶M. A. Z. Hasan, "The flow over a backward-facing step under controlled perturbation: Laminar separation," *J. Fluid Mech.* **238**, 73 (1992).
- ²⁷R. A. Petersen and R. C. Clough, "The influence of higher harmonics on vortex pairing in an axisymmetric mixing layer," *J. Fluid Mech.* **239**, 81 (1992).
- ²⁸J. T. Stuart, "Nonlinear effects in hydrodynamic stability," in *Proceedings of the 10th International Congress on Applied Mechanics*, edited by F. Rolla and W. T. Koiter (Elsevier, New York, 1962), pp. 63–97.
- ²⁹J. T. Stuart, "On the nonlinear mechanics of hydrodynamic stability," *J. Fluid Mech.* **4**, 1 (1958).
- ³⁰D. R. S. Ko, T. Kubota, and L. Lees, "Finite disturbance effect in the stability of laminar incompressible wake behind a flat plate," *J. Fluid Mech.* **40**, 315 (1970).
- ³¹S.-S. Lee and J. T. C. Liu, "Multiple large-scale coherent mode interactions in a developing round jet," *J. Fluid Mech.* **248**, 383 (1993).
- ³²M. E. Goldstein and S. J. Leib, "Nonlinear roll-up of externally excited free shear layers," *J. Fluid Mech.* **191**, 481 (1988).
- ³³M. E. Goldstein and L. S. Hultgren, "Nonlinear spatial evolution of an externally excited instability wave in a free shear layer," *J. Fluid Mech.* **197**, 295 (1988).
- ³⁴L. S. Hultgren, "Nonlinear spatial equilibration of an externally excited instability wave in a free shear layer," *J. Fluid Mech.* **236**, 635 (1992).
- ³⁵F. O. Thomas and H. C. Chu, "An experimental investigation of the transition of a planar jet: Subharmonic suppression and upstream feedback," *Phys. Fluids A* **1**, 1566 (1989).
- ³⁶P. Freymuth, "On transition in a separated laminar boundary layer," *J. Fluid Mech.* **25**, 683 (1966).
- ³⁷Y. Zohar and C. M. Ho, "Dissipation scale and control of fine-scale turbulence in a plane mixing layer," *J. Fluid Mech.* **320**, 139 (1996).
- ³⁸J. T. Stuart, "On the nonlinear mechanics of wave disturbances in stable and unstable parallel flows. Part I. The basic behavior in plane Poiseuille flow," *J. Fluid Mech.* **9**, 353 (1960).
- ³⁹A. Alper and J. T. C. Liu, "On the interactions between large-scale structure and fine grained turbulence in a free shear flow. II. The development of spatial interactions in the mean," *Proc. R. Soc. London, Ser. A* **395**, 497 (1978).
- ⁴⁰J. T. C. Liu and H. T. Kaptanoglu, "Control of free shear layers," AIAA Paper No. 87-2689, 1987.
- ⁴¹R. R. Mankbadi, G. Raman, and E. J. Rice, AIAA Paper No. 89-0906, 1989.
- ⁴²R. R. Mankbadi, "Multifrequency excited jets," *J. Fluid Mech.* **160**, 385 (1991).
- ⁴³I. Wygnanski, D. Oster, H. Fiedler, and B. Dziomba, "On the perseverance of a quasi-two-dimensional eddy structure in a turbulent mixing layer," *J. Fluid Mech.* **93**, 325 (1979).
- ⁴⁴D. G. Crighton and M. Gaster, "Stability of slowly diverging jet flow," *J. Fluid Mech.* **77**, 397 (1976).
- ⁴⁵N. Itoh, "Nonlinear stability of parallel flows with subcritical Reynolds numbers. Part I: An asymptotic theory valid for small amplitude disturbances," *J. Fluid Mech.* **82**, 455 (1977).